SEMMELWEIS EGYETEM

DOKTORI ISKOLA

Ph.D. értekezések

3198.

Brachyahu Meir Kestecher

Humán molekuláris genetika és géndiagnosztika

című program

Programvezető: Dr. Wiener Zoltán, habilitált egyetemi docens

Témavezető: Dr. Osteikoetxea Vélez Xabier, tudományos főmunkatárs

The effects of hypercholesterolaemia and atherosclerosis on circulating CD63+ extracellular vesicle levels

PhD thesis

Brachyahu Meir Kestecher

Semmelweis University Doctoral School

Molecular Medicine Division

Supervisor: Dr. Xabier Osteikoetxea, PhD

Official reviewers: Dr. Zoltán Varga, PhD

Dr. Anikó Görbe, PhD

Head of the Complex Examination Committee: Prof. Attila Tordai, DSc

Members of the Complex Examination Committee: Dr. Viola Tamási, PhD

Dr. Krisztina Takács, PhD

Budapest

2025

Table of Contents

List of Abbreviations

ABB	Annexin binding buffer
ACD-A	Anticoagulant citrate dextrose solution A
ACVD	Atherosclerotic cardiovascular disease
ApoB	Apolipoprotein B
ApoE	Apolipoprotein E
CVD	Cardiovascular disease
E/e' ratio	Ratio of early diastolic mitral inward flow velocity to early diastolic mitral annulus velocity
eGFR	Estimated Glomerular Filtration Rate
EGM2	endothelial cell growth media-2
EV	Extracellular vesicles
GOT	Glutamate oxaloacetate transaminase
GPT	Glutamate pyruvate transaminase
HbA1c	haemoglobin A1c
HDL	High-density lipoprotein
HDL-C	High-density lipoprotein cholesterol
HFD	High fat diet
HUVEC	Human umbilical vein endothelial cell
ISEV	International Society for Extracellular Vesicles
IVD	In vitro diagnostics
KO	Knock out
lEV	Large extracellular vesicles
LDL	Low-density lipoprotein
LDLR	Low-density lipoprotein receptor
LDL-C	Low-density lipoprotein cholesterol
LOX-1	Lectin-like oxidized low-density lipoprotein receptor-1
LPS	Lipopolysaccharide
LRP1	Lipoprotein receptor-related protein-1
LVRi	Left ventricular remodelling index
LVAWTd,	Left ventricular anterior wall thicknesses in diastole
LVPWTd	Left ventricular posterior wall thicknesses in diastole

LVEDD	Left ventricular diameters in end-diastole
LVESD	Left ventricular diameters in end-systole
LVEDV	Left ventricular end-systolic volumes
LVESV	Left ventricular end-diastolic volumes
LVSV	left ventricular stroke volume
mEV	Medium extracellular vesicle
MI	Myocardial infarction
MISEV	Minimal information for studies of extracellular vesicles
NTA	Nanoparticle tracking analysis
Ox-LDL	Oxidised Low-density lipoprotein
PBS	Phosphate-buffered saline
PCSK9	Proprotein convertase subtilisin/kexin type 9
PFP	Platelet free plasma
PPP	Platelet poor plasma
qPCR	Quantitative/real time PCR
RWT	Relative wall thickness
SCARB-1	Scavenger receptor class B type 1
sEV	Small extracellular vesicle
TC	Total cholesterol
VLDL	Very Low-density lipoprotein
WT	Wild type

Introduction:

As the population of aging communities increase globally, the incidence of atherosclerotic cardiovascular disease (ACVD) has emulated this increase, making ACVD the leading cause of deaths not just in western populations, but worldwide (1). Predominantly, these fatalities occur from plaque obstructions to the coronary artery leading to acute myocardial infarction (MI) (2, 3), with carotid and cerebral arterial blockages causing stroke related deaths (4), making them the second and third highest levels of vascular fatalities respectively (4). Other issues caused by atherosclerosis include peripheral artery disease, which often leads to limb and organ threatening damage (5). Low-density lipoprotein (LDL) and oxidised-LDL (ox-LDL) are key biomarkers in all forms of sclerotic vascular disease, making LDL a good prognostic tool and therapeutic target for ACVD genesis and development, currently being utilised by clinicians globally (6, 7). It is important to note that LDL has a long history in aiding diagnostics, prognostics and drug development for patients with suspected arterial plaque formation (8), with known links dating back to as early as 1913 (9). Higher levels of circulating LDL leads to increased endothelial internalisation of LDL to the sub-endothelial space where LDL can undergo oxidation ox-LDL. ox-LDL is recognised by the immune system which in-turn causes monocyte recruitment to the endothelium, ultimately migrating the subendothelial space where they can differentiate to macrophages. These macrophages will then commence the process of ox-LDL engulfment, eventually further differentiating them to foam cells, increasing fatty deposits, and forming fatty streaks on arterial walls (10). This process marks the beginning plaque formation, a process that often silently develops over several decades, frequently leaving the victim unaware of the ever-constricting artery until a life-threatening incident occurs leaving a lifelong or terminal injury to the patient. Whether or not a patient survives the initial attack (MI or stroke), the susceptibility to subsequent disease and lower life expectancy are well established. Making this topic of vital importance for further investigation. From early detection of plaque formation, treatment to stabilise patients at risk, to reversibility of the damage already caused, are all key areas of research still to be discovered.

Extracellular vesicles (EVs) are small, membrane-bound particles released by all known cell types into the extracellular environment. They play an essential role in cell-to-cell communication by carrying a variety of biomolecules, including proteins, lipids, and

nucleic acids, which can then be transported to other cells. This transfer of materials allows EVs to influence a wide range of biological processes, from immune responses to tissue repair and even cancer suppression (11-13). EVs are released from all known cell types carrying markers and macromolecules of their host, sending out vital information on the status of the cell whether healthy or in distress. EV uptake from the extracellular matrix may occur at random to nearby cells if the EV-associated tetraspanins (e.g. CD9, CD63, or CD81) are abundant on their surface, or via other methods such as, clathrin-mediated, caveolin-mediated, and lipid raft endocytosis (14) as well as macropinocytosis, and phagocytosis. Some EVs could carry specific cargo and might have distinctive markers on their surface, which may be used as signalling molecules or to target more specialised cell types and tissue (15).

There are several types of EVs, classified based on their size, location of origin, and their biogenic pathway. According to the latest Minimal information for studies of extracellular vesicles (MISEV) 2023 guidelines set out by the International Society for Extracellular Vesicles (ISEV) (16) there are 2 major categories of EVs, large-EVs (lEVs) and small-EVs (sEVs). lEVs are now classed as vesicles with a diameter ≥ 200 nm, whilst sEV are those EVs with diameter ≤ 200 nm. According to older nomenclature and guidelines, the sizes were previously considered in three categories, with < 100 nm considered sEVs, 100 – 1000 nm as medium EVs (mEVs), and 1-5 μm considered lEVs (17). In older versions of nomenclature and terminology used in the field, sEVs were synonymous with exosomes, mEVs synonymous with microvesicles or microparticles, and lEVs corresponded to apoptotic bodies (18), although even back then these terms were somewhat debated.

Since 2014, more data has shown that not all multivesicular body originating EVs are of the same or even similar size (19, 20). Therefore, to consider an EV an “exosome” or a “microvesicle”, it is now necessary to prove the biogenesis and method of EV release. The third category often mentioned are “apoptotic bodies”, formally considered the largest of the EV sub-populations, however, dying cells have now been shown to produce EVs of a diverse size (21, 22) in the apoptotic process. It is therefore now required to show that such EVs were released as a part of the programmed cell death if suggesting them as apoptotic bodies.

Figure 1 below, adapted from Brezgin et. al. 2024 (23) shows the different EV release mechanisms that more clearly define the nomenclature of some of the EV subtypes. It is also noteworthy, that at this point in time we do not have a method to completely isolate a particular subtype of EVs, but enrichment particular EVs is becoming more common and induction of a particular EV release mechanism (e.g. inducing apoptosis in cells using FasL, or Fas ligand) is also possible in order to study a particular form of EVs.

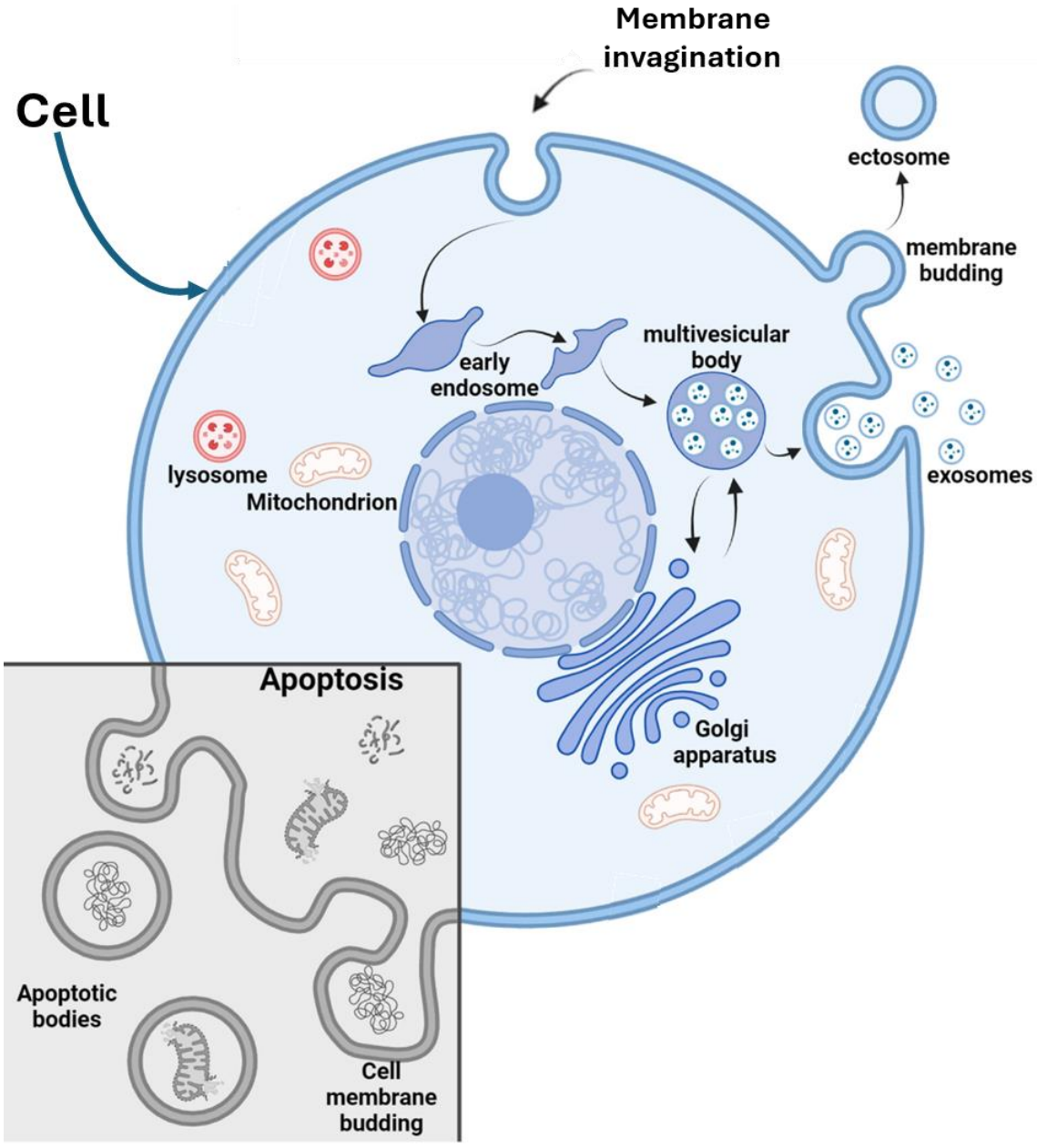

Figure 1. This schematic is a visual representation of the different mechanisms of extracellular vesicle release from cells. At the top centre, we show the endocytic invagination of extracellular macromolecules, this leads to the endosomal pathway, and

after endosomal escape, the multivesicular body formation can occur – which intern leads to the release of exosomes. Top right of the schematic, the budding and release of ectosomes can be seen. At the bottom left of the image the process apoptosis can be seen, starting with the blebbing of the cell membrane, protrusions, and finally the release of apoptotic bodies. This last method of EV release also often contains fragmented DNA and other clear signs of its mechanism of release. This image is an adaptation of Figure 1 published by Sergey Brezgin et. al. in 2024 (23).

An additional method of EV classing can be done through surface marker characterisation. By showing that an EV or EV population are rich in a particular marker will often be used to determine the pathway of its genesis as well as the tissue of origin or releasing cell type. One universal marker that many EV researchers still utilise today, in order to show that biological isolates are in fact EVs, is phosphatidylserine. Phosphatidylserine is typically found in the inner cell membrane, meaning cells will not likely show its presence unless lysed or undergoing apoptosis. During budding and release of EVs, membrane flipping occurs, allowing phosphatidylserine (among other inner membrane phospholipids) exposure on the EV surface. Annexin V in the presence of calcium will bind phosphatidylserine. When biological isolates bind to annexin V in the presence of calcium, this is enough to show (at least for pilot studies) that EVs are present in the mix.

Figure 2 below shows some of the basic EV markers which are used to identify vesicle populations in either biofluids or EV isolates in buffer.

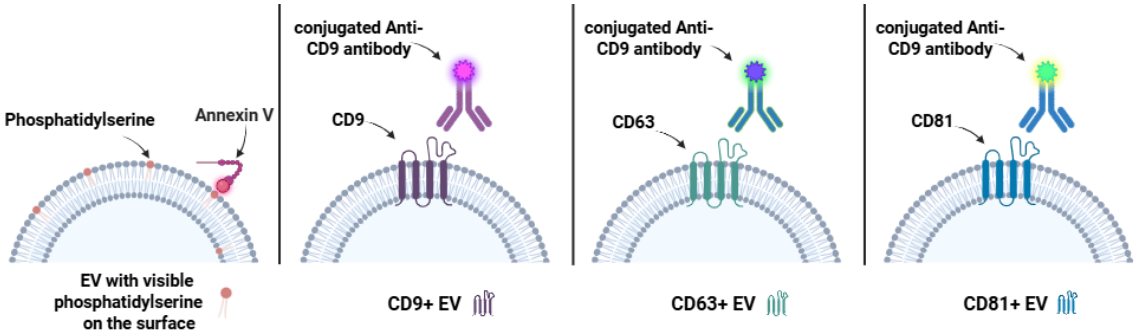

Figure 2. A schematic diagram showing the markers and antibodies found on the surface of extracellular vesicles (EVs), which can be used to determine whether a particular population are vesicles or not, while also serving to give a rough estimate into the likely biogenic pathway of the population. On the left, phosphatidylserine can be seen and are

likely present on all EVs. Centre left, and centre right are CD9 and CD63 and associating antibodies, these EVs are likely of endosomal origin. To the right, CD81 plus its antibody can be seen, these are likely membrane budding EVs.

As briefly mentioned above, many common proteins including tetraspanins on the cell surface will end on the surface of EVs. Tetraspanins are a family of membrane proteins, characterized by four transmembrane domains, typically two extra-membranous loops and shorter inter-membranous tail ends. Tetraspanins are involvement in various cellular processes such as trafficking, adhesion, and cellular signalling. As with all cellular processes, different tetraspanin subtypes may have distinct features in order to perform more specialised tasks. CD9, CD63, and CD81 are among the most common tetraspanins found on the surface of our EVs. CD63 for example, is abundantly found and detected on the surface of EVs. CD63 is particularly enriched in endosomal membranes making them largely specific to exosomes, one of several subtypes of EVs originating from the endosomal and late endosomal pathways. It is important to mention however, that as CD63 is also found on the cell surface, not all CD63+ EVs originate from the endosome, and thus does not directly classify them as exosomes.

CD63 is often used as a biomarker for the detection and characterisation of EVs. For these reasons, both in research and in a clinical context, CD63 is employed in several methods for EV detection and isolation, including, flow cytometry, western blot, immune bead capture and immune-labelling microscopy (confocal imaging).

As EVs are so abundantly released from cells, EVs are found in all body fluids that have been studied to date, including blood, saliva, urine, and cerebrospinal fluid among others. Based on the relative size of many EVs, unlike cells and other larger biomaterial, they can easily pass the blood-brain barrier. As such, they make exceptional tools and can be exploited for liquid biopsies, rather than more traditional invasive and complex tissue biopsies. This has made them very attractive to clinicians across many fields and a potential gold mine for biological and pharmacological researchers alike.

Over the last decade or more EVs have slowly been gaining traction in a multitude of biological and medical investigations (24) due to emerging evidence of their involvement in vast numbers biological and physiological pathways (25-27) allowing for speculation of their association to disease. As predicted, EVs have been shown more recently to be

involved in pathogenic processes both *in vivo* and *in vitro*, particularly in the field of oncology (27, 28) and cardiovascular diseases (CVD) (25). Lately, EVs have also shown strong potential as therapeutic agents for many diseases (29) including a variety of cardiovascular related health detriments (30, 31). This phenomenon has made EVs a leading area of interest to many clinicians as well as pharmacists for drug development (32-34).

Contemporary diets are often based on high fatty content including "fast foods" as well as heavily processed high cholesterol products which are still noted for their contribution to dysfunction of cholesterol and lipoprotein metabolism which can often lead to ACVD (35, 36). Such diets are also shown to have notable involvement of obesity, MI, stroke, and diabetes (36, 37) and are even believed to play a crucial role in many other co-morbidities such as cancer (38). Being that an increase in cholesterol has been historically noted as associated with poor diet (39, 40), our investigation involved using a high fat diet (HFD) in mice models to assess the cholesterol changes and how such alterations would affect circulating EV levels.

As seen in clinical settings, ACVD predominantly occurs in midlife and older patients (41).For this reason, this research also elected to include an old age condition, whereby mice were left to grow old under regular maintenance in the animal care facility. As seen below a big part of our *in vivo* study focused on mouse models, with a KO of different cardiovascular related genes. Due to the increasing awareness in recent years of the impact genetics plays as a primary cause in cholesterol dysregulation (42, 43), and with a growing number of publications alluding to genetics as primary cause of ACVD, we also used lipoprotein related genetically modified animal models to investigate cholesterol dysfunction, dyslipidaemia and atherosclerosis. After the establishment of disease states, we were then able to assess other suspected biomarker alterations associated with ACVD. Mainly, EVs and certain EV-sub populations.

The motivation for the current research came when in 2016, our laboratory demonstrated the association and co-isolation of LDL and EVs from human blood plasma (44). Previously thought to be unrelated, with suspected divergent densities, biogenic pathways and metabolic properties, this paper was a shock not only to the young EV field, but also to the veterans of the well-established lipoprotein academics. Since then, other groups

have continued to show the association of EVs and other lipoproteins including, high-density lipoprotein (HDL), LDL, and very lower-density lipoprotein (VLDL) amongst others (45, 46) and continue to show lipoprotein contamination in EV preps from all tissue and body fluids regardless of the isolation methods applied (45). Figure 3 below is an image taken from the Soda Barbara et. al 2016 publication (44) from our lab. This is a transmission electron microscopy image which shows association of both EVs and LDL particles in the same isolate. It can also be seen from the image that the two distinct populations associate fairly well.

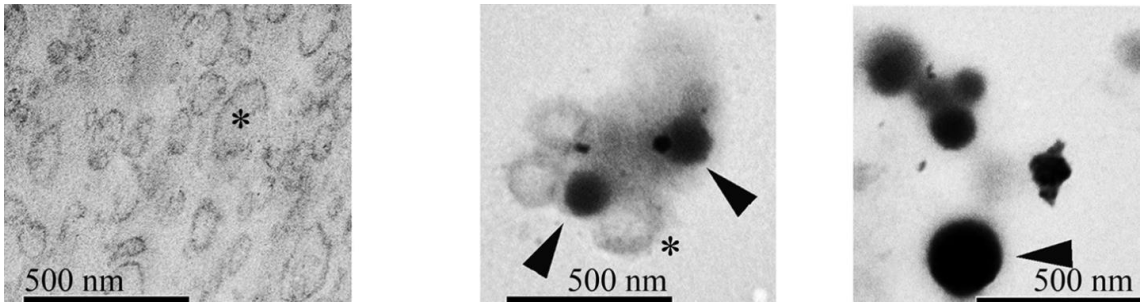

Figure 3. All three images are transmission electro micrographs taken from figure 3 of the 2016 publication from our lab. The left hand side image is an ultrathin section prepared from PFP-derived large extracellular vesicles (lEVs) (back then known as microvesicles or medium sized EVs) pellet. The asterisk represents what are now considered lEV. The two images to the right side of the figure are both similar micrographs after osmification, allowing the electron dense lipoproteins (black arrows) to be visualised. Here too, the asterisk represents lEVs (44).

A recent review on the topic of EVs involved in therapeutic applications made a primary focus on the interaction that EVs have with lipoproteins (47). This paper highlights the prospective use of EVs as a therapeutic option for vascular and other cholesterolaemic related disorders. Figure 4 below used in the above-mentioned review (47) shows two diagrams - both showing the magnitude of overlapping proteins which are associated with both lipoproteins and EVs. This figure once again shows the overlap between the two fields and indeed the difficulties of separating and distinguishing EVs from lipoproteins.

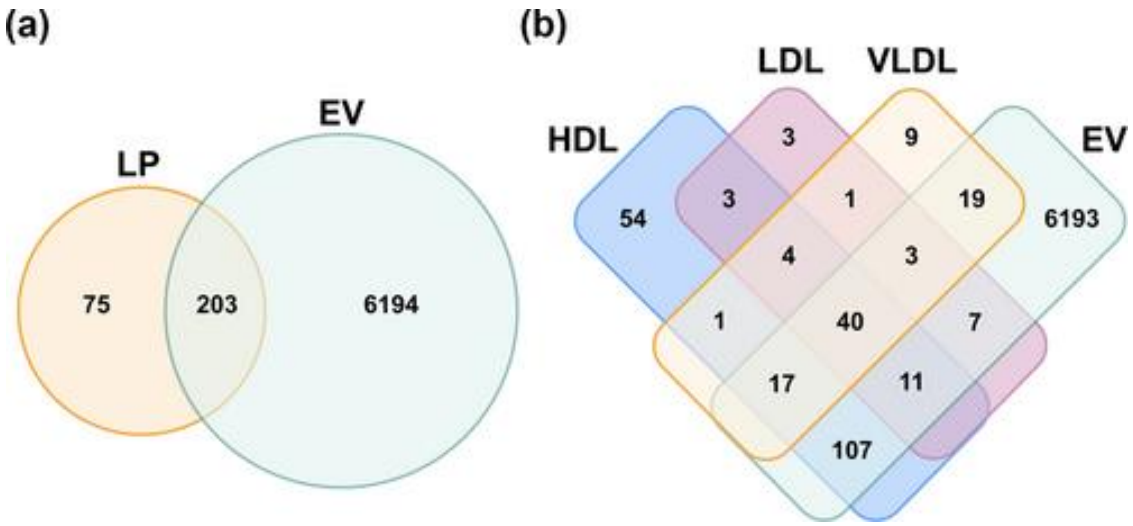

Figure 4. The protein composition and proteomic overlap between lipoproteins and extracellular vesicles (EVs). **a** Based on a 2021 meta-analysis (48) which considered > 6,000 proteins from both EVs and lipoproteins, they shared at least 203 proteins. **b** Here it can be seen using a Venn diagram the individual lipoprotein-proteins which are also associated with EVs. Here it can be seen that EVs share 79 proteins with very low-density lipoproteins, 61 with low-density lipoprotein, and 175 shared proteins with high-density lipoprotein. This figure was produced by the authors of the recent review on therapeutic and pharmacological applications in EV (47).

Many of these earlier studies gave way to other hypothesis' and later the discovery of the protein corona on the surface of EVs (49). Based on this, we hypothesized that EVs may also play a crucial role in atherosclerosis development, possible affecting cellular internalisation of cholesterol in monocytes as well as macrophages. This internalisation of cholesterol causes foam cell formation, and endothelial tissue fatty streaks in the initial stage of arterial plaque build-up.

The LDL receptor (LDLR) is a crucial regulator of LDL-cholesterol (LDL-C) involved in LDL clearance from blood circulation through guided cellular internalisation for degradation (50) and transport to the liver. Due to our comprehension of the clinical implications of the LDLR, we postulated the potential roles the LDLR may play in regulating circulating EV levels. We utilised this in studying how EV levels may up- or down-regulate LDL metabolism. Other researchers have previously opted for downregulation of or even knock-out (KO) of the LDLR gene, to study the biological effects and clinical implications this may have of total cholesterol (TC) and LDL-C levels

(51, 52) in circulation in addition to the cellular impact this gene and associated proteins may influence. However, in this research we have also elected to explore these roles, as well as the potential role the LDLR gene plays in determining EV levels as well as, in cardiac function, and in atherosclerosis development in murine models.

An additional gene of high relevance in ACVD, is proprotein convertase subtilisin/kexin type 9 (PCSK9), which serves as a negative regulator of LDLR, which has also become a key therapeutic target to help regulate LDL-C levels in patients with more severe forms of clinical hypercholesterolaemia (53, 54). Although much of the work in understanding the PCSK9 gene and its resulting protein is yet to be understood, various inhibitors have been readily available and authorized for clinical use to help reduce LDL-C levels in chronic hypercholesterolaemic and ACVD patients for several years now (55), with FDA approval being granted in 2015 (56). The preparation stages are currently in progress for deletion of the PCSK9 gene employing CRISPR/Cas9 technology, which could be used in the future in humans. The clinical use of this technology will specifically target hepatic cells (57) were LDLR function is paramount. Based on the significant clinical interest in PCSK9 and its direct corelation to circulating LDL levels, this study also opted to examine circulating EV levels in a $PCSK9^{-/-}$ murine model.

For the aforementioned reasons, we elected to study C57BL/6J background mice, with either $PCSK9^{-/-}$ and $LDLR^{-/-}$ plus a wild-type (WT) control group. We studied an $LDLR^{-/-}$ mouse model where EV changes occurring in an increased LDL-C environment could be observed and a $PCSK9^{-/-}$ mouse model, where EV investigations could take place in a reduced cholesterol setting. Some studies show that hypocholesterolaemia can have a genetic contributing factor (58) while others show poor diet has a role in increased cholesterol levels (36). Although both may have their own role in increasing LDL levels, it is established that high circulating LDL-C is an indicator of poor cardiovascular prognosis in humans, with increased risk of atherosclerosis (59). Therefore, this study also evaluates the circulating EV levels in human platelet free plasma (PFP) from normal and hypercholesterolaemia patients to understand how EV levels may be relevant in clinical atherosclerosis and patient cardiovascular health.

Being that previous research has shown that EVs and lipoproteins are inseparable in bodily fluids (44) using even the most cutting-edge technology for isolation (60) and that

such complexes form spontaneously and rapidly when co-incubated (44) it is evident that EVs play a crucial role in many or even perhaps all functions of lipoproteins including LDL-C. It has long been reported that cholesterol levels, mainly LDL-C, are an important prognostic marker heavily involved in atherogenesis. Based on the current literature regarding the EV-lipoprotein relationship, including previous work from our own lab as well as the work of other research groups, we theorized that EVs are involved in hypercholesterolaemia and atherogenesis. It appears that there is a lack of information currently available as to the direct mechanism of EV-lipoprotein binding. Although the leading conjecture is that binding occurs through the protein corona on the EV surface (49) (depending on size, charge, and surface chemistry of both particles). It is also not known which EVs are more likely to bind cholesterol, or which may more specifically bind LDL-C. Here, we aim to identify circulating levels of EV subpopulations in blood plasma with normal, high or low LDL levels in mice and humans. The current study sheds light on EV subpopulations likely to be involved in hypercholesterolaemia and atherogenesis based on size and surface markers. And may even offer an explanation as to the mechanisms by which EVs might protect against or exacerbate ACVD. Based on the established interplay between EVs and lipoproteins we hypothesize that concentration of large EVs with particular surface markers will be a good predictor of ACVD and may be used prognostically in clinics in the future.

2. Objectives:

Our principal objectives in this work were as shown below.

- To investigate the relationship between circulating EVs, particularly lEVs, and lipoproteins (primarily LDL).

- To explore whether circulating lEV subpopulation levels are associated with the presence, and correlate to the extent of atherosclerosis.

- To examine how circulating lEV subpopulation levels vary with age in-vivo.

- To assess the potential of CD63+, CD81+, and annexin V+ lEVs as prognostic biomarkers for ACVD, as well as to consider how aging may impede this correlation.

3. Methods:

3.1 Mice handling

All experimental procedures on mice adhered to the guidelines set by the Council Directive of the European Union (86/609/EEC), with approval from the Institutional Animal Care and Use Committee of Semmelweis University (PE/EA/1363-8/2019) obtained prior to the experiments. Male mice with a C57BL/6J background, aged 10 weeks, and of wild-type (WT), PCSK9$^{-/-}$, and LDLR$^{-/-}$ genotypes were used, with six mice in each genetic background. The mice were supplied by the Jackson Laboratory (JAX catalogue numbers: 000664, 005993, and 002207, Bar Harbor, USA) and were housed at the animal facility of the Institute of Genetics, Cell- and Immunobiology.

The animals were maintained on a standard 12-hour light/dark cycle with unrestricted access to food and water. At the beginning of the experiment (week 10), blood samples were collected from the retrobulbar venous plexus while the animals were on a normal diet. In the second week (11 weeks of age), following a 5-hour fast, blood was again collected from the retrobulbar venous plexus, after which the mice were placed on a high-fat diet (HFD) containing 45% kcal from fat (catalogue # D12451, Research Diets, New Brunswick, USA) for a period of 12 weeks (until reaching 23 weeks of age).

At the midpoint of the HFD regimen (week 6 of HFD, age 17 weeks), mice were fasted for 5 hours, and blood was again collected from the retrobulbar venous plexus. At the end of the 12-week HFD period (age 23 weeks), mice were anesthetized with isoflurane (1 mL/100 g body weight) and euthanized via terminal blood collection from the inferior vena cava. Weekly weight measurements were recorded from 10 to 23 weeks of age.

To evaluate the effects of aging, male WT, PCSK9$^{-/-}$, and LDLR$^{-/-}$ mice (all C57BL/6J background) were kept on a regular chow diet for 22 months, with group sizes of six. At 22 months, surviving mice were anesthetized with isoflurane (1 mL/100 g body weight) and euthanized via terminal blood collection from the inferior vena cava, with body weights measured at the time of sacrifice. Figure 5 below is a schematic, showing the outline of the experimental design for all the *in vivo* work carried out in this project.

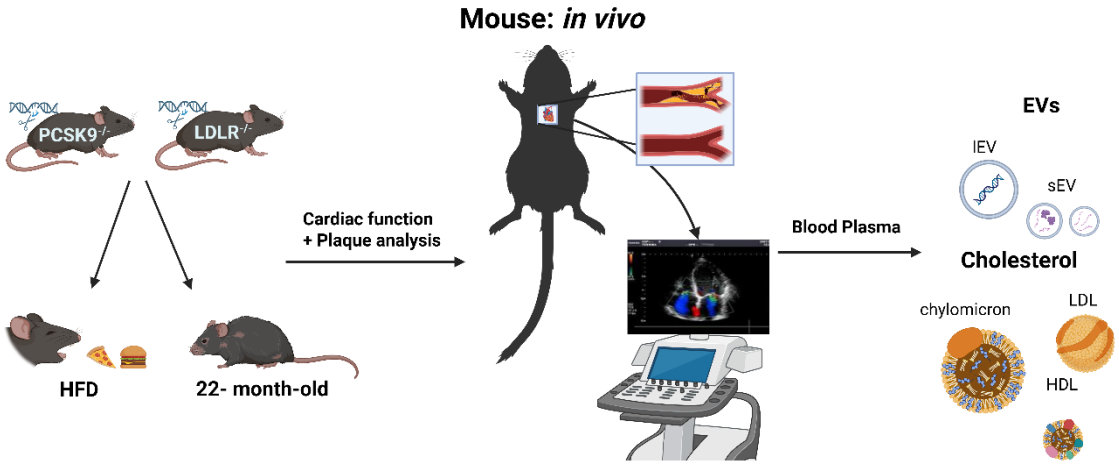

Figure 5. This is a basic schematic representation of the *in-vivo* work performed in this project. As can be seen on the left, mouse models with the cardiovascular related genes PCSK9 and LDLR knocked out were either fed high-fat diet for 12 weeks or left to grow old. At experimental end (as seen in the centre), cardiac measurements were taken and animals were euthanised, after which tissue collection and plaque analysis was performed. Blood plasma was used later to assess cholesterol and extracellular vesicle levels.

3.2 Mice genotyping

Genotyping of mouse strains was routinely conducted every 12–18 months or whenever new breeding cages were established to confirm the homozygosity of breeding pairs and their offspring. Typically, two females and one male from each knockout (KO) strain were genotyped simultaneously, along with 1–2 wild-type (WT) animals included as negative controls. A DNA ladder (catalogue # SM0373, Thermo Scientific, Waltham, USA) with 50 bp was utilized. PCR primers and protocols provided by the Jackson Laboratory were followed. For PCSK9$^{-/-}$ mice, genotyping was performed using protocol 27858: Standard PCR Assay - Pcsk9<tm1Jdh> Version 4.2, while for LDLR$^{-/-}$ mice, protocol 27075: Standard PCR Assay - Ldlr<tm1Her>-alternate 1 Version 1.2 was used.

3.3 Human samples

In this study, PFP samples were collected from clinical patients. Blood samples were obtained from venous blood drawn from patients admitted to the Városmajor Clinic at Semmelweis. Blood collection tubes were anticoagulant citrate dextrose solution A

(ACD-A) containing tube (15% ACD-A). These patients had been evaluated and cleared of acute cardiac ischemic events after presenting with chest pain in the emergency department. The study received ethical approval from the Regional and Institutional Committee of Science and Research Ethics at Semmelweis University (67/2022). Samples included male patients, with their data summarized in Table 1. Group A consisted of patients with normal cholesterol levels, while Group B included patients with hypercholesterolemia (n=6 per group). Total cholesterol (TC), LDL-C, high-density lipoprotein cholesterol (HDL-C), triglycerides, glucose, and haemoglobin A1c (HbA1C) were measured using the DxC 700 AU (Beckman Coulter, Brea, USA). Figure 6 below is a basic schematic, outlining the experimental design for all the clinical measurements we performed.

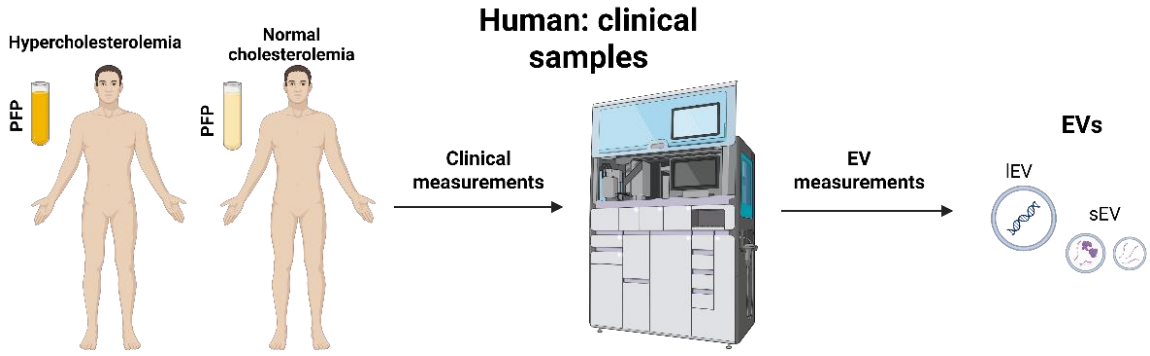

Figure 6. A schematic representation of the clinical investigation performed in this research. Here, patient blood was taken from both patients with normal cholesterol and those with high cholesterol levels. Blood biomarkers relevant to cardiovascular diseases was assessed by the clinic. Upon receipt, we investigated the EV content of the plasma from both patient groups.

Table 1. The above table shows the data collected from two groups of patients. The first group are of patients with normocholesterolaemia and the second group are patients with hypercholesterolaemia. A numbering system used to randomize the patients in each group, and anthropometric data providing sex and age of the patients recruited. The date of recruitment of each patient is provided. A lipid profile including total cholesterol, low-density lipoprotein, high-density lipoprotein, and triglycerides is included in this table. Additional data provided here includes levels of, glucose, HbA1c, estimated Glomerular Filtration Rate (eGFR), glutamate oxaloacetate transaminase (GOT), and glutamate

pyruvate transaminase (GPT). For each row where measurements are shown, an unpaired t-test is displayed, with the last column showing the whether the groups are significantly altered. Table adapted from supplementary data (61) of authors own first author publication.

Cholesterolaemic groups	No.	Antropometric data		Time of recruitment	Lipid profile				Other lab data				
		Sex	Age		Total chol	LDL	HDL	TG	Glucose	HbA1C	eGFR	GOT	GPT
Normo	7	M	39	01/02/2022	4.7	3.06	0.92	1.51	7.4	-	90	33	58
	27	M	24	07/02/2022	4.8	2.92	1.77	0.2	5.6	5.2	90	25	25
	28	M	35	07/02/2022	4.3	2.49	1.56	1	5.5	5.3	90	23	18
	34	M	25	14/02/2022	4.1	2.17	1.86	0.7	5.3	-	90	21	12
	41	M	58	17/02/2022	3.6	1.65	1.81	0.7	6.4	-	82.6	24	25
	69	M	63	29/03/2022	4.6	3.01	0.88	3.1	5.5	5.7	90	22	18
Hyper	13	M	39	01/02/2022	6.6	3.26	2.9	1.2	5	5.1	90	35	22
	15	M	32	01/02/2022	5.5	3.04	1.8	1.45	4.6	5.2	87.7	27	27
	24	M	48	04/02/2022	6.6	4.65	1.09	2.8	5.2	-	81.8	37	45
	30	M	62	27/02/2022	7.2	4.76	1.59	1.6	N/A	5.5	5.1	50	100
	48	M	38	01/03/2022	7.5	4.29	2.23	3.7	5.1	4.9	90	19	15
	67	M	52	29/03/2022	6.8	4.75	1.41	1.6	10.2	6.6	88	44	74
unpaired t-test p value			0.59		3.69E-05	0.0024	0.2768	0.169	0.94654	0.8902	0.304	0.0549	0.1942
Significantly different?			no		yes	yes	no	no	no	no	no	no	no

3.4 Mouse blood collection, handling, and storage

Blood collection was performed via the retrobulbar venous plexus with the use of Corning® Pasteur pipettes L 5 3/4 in. (146 mm), standard tip (catalogue # CLS7095B5X-1000EA, Merck Sigma, Darmstadt, Germany) whenever mice blood was extracted, except for when sacrificing the mice. During animal sacrifice, blood was drawn from the inferior vena cava using ACDA-laced syringe and needle for precise extraction. Each blood sample was lightly mixed with 15% ACD-A anticoagulant, kept at 4 °C, and processed within two hours of collection. Samples were centrifuged at 2,500 g for 15 minutes at 4 °C to obtain platelet-poor plasma (PPP), which was carefully separated from the red blood cells. A 45 µL aliquot of PPP was reserved at 4 °C for later assessment of cholesterol. For downstream EV measurements, the remaining PPP was centrifuged again at 2,500 g for 15 minutes at 4 °C to separate PFP. This PFP was then aliquoted into 1.5 mL Eppendorf tubes and diluted 1:1 with 0.1 µm-filtered saline (0.9M NaCl) solution. The saline diluted PFP was flash-frozen in liquid nitrogen and stored at -80 °C.

3.5 Assessment of cardiovascular function

All cardiovascular parameters performed on mice were assessed at the end date of experimental timeline, as previously described (61, 62). Briefly, a Vevo 3100 high-resolution *in vivo* imaging system (Fujifilm VisualSonics, Toronto, Canada) was used with an ultrahigh frequency transducer (MX400, 30 MHz, 55 fps) and evaluation was performed using VevoLAB software (version 5.6.1, Fujifilm VisualSonics, Toronto, Canada). Animals were anesthetized with isoflurane (for induction: 5 V/V% in O_2; for maintenance: 2 V/V% in O_2), with spontaneous breathing. Throughout the echocardiographic measurements, body temperature was kept at 37±0.5°C, and electrocardiographic activity was obtained continuously.

Chest hair was removed, and two-dimensional cines were obtained from the long-, short-, and apical four-chamber views of the heart (LAX, SAX, and APIC4, respectively). Left ventricular end-systolic and end-diastolic volumes (LVESV and LVEDV, respectively, derived from the rotational volumes of the left ventricular trace at diastole and systole, around the long axis line of the spline), left ventricular stroke volume, left ventricular ejection fraction and cardiac output measurements were obtained from the LAX view.

Left ventricular diameters in end-diastole and end-systole (LVEDD and LVESD, respectively), left ventricular fractional shortening, left ventricular mass, and left ventricular anterior or posterior wall thicknesses in systole and diastole (LVAWTs, LVAWTd, LVPWTs, and LVPWTd, respectively) were acquired from the SAX view. Relative wall thickness was calculated as 2*LVPWTd/LVEDD; left ventricular remodelling index was calculated as left ventricular mass/LVEDD. Iso-volumetric relaxation time, and E/e' ratio (where E: peak transmitral blood flow velocity in early diastole measured by pulsed wave Doppler imaging; and where e': mitral annular velocity in early diastole assessed by tissue Doppler imaging) were derived from the APIC4 view, indicative for diastolic function.

3.6 Quantification of atherosclerotic plaques

After termination of the mice, the aortic arches were carefully and precisely isolated, including removal of any visceral tissue using a stereomicroscope. An earlier protocol was followed (63) in order to stain and then image the isolated arches. Briefly, aortic

arches were stained with Oil-Red-O (Catalogue #31170, Serva, Heidelberg, Germany). A 70% ethanol wash was applied before staining and an 80% ethanol wash afterward. Stained specimens were stored in 1x phosphate-buffered saline (PBS) until imaging, which was performed using the S9D microscope with objective lens 10450528 and a FLEXACAM C1 camera (Leica, Wetzlar, Germany).

The stained area of each plaque, represented as the Oil-Red-O+ area/whole tissue ratio (%), was analysed with offline downloaded version (1.49) of ImageJ. Using the Wand tool, the total area of the isolated whole tissue was selected and measured. The following steps were employed to identify plaques in each isolated aortic arch:

- Under the "Image" tab, "Colour" and then "Split Channels" were selected.
- In the "Process" tab, the "Image Calculator" was used to subtract red from green.
- In the "Image" tab, the "Adjust" function was selected to set a threshold for Oil-Red-O+ particles (thresholds were visually confirmed by two independent researchers).
- The "Process" tab was used again to apply a watershed to the image of Oil-Red-O+ particles by selecting "Binary" and then "Watershed."
- Total particle area was then calculated using the "Analyse" tab and then selecting "Measure Particles," using the prompt "0-infinity, 0.0-1.0" to measure all stained particles of any shape or size.

All images and groups were initially randomized and blinded by one researcher before being independently analysed by two additional researchers. After which, the images were de-coded by the initial researcher to analyse the results for each group.

3.7 Mice cholesterol level measurements

Measurements were conducted using a Quantitation Kit for HDL and LDL/VLDL (catalogue # MAK045-1KT, Merck Sigma, Darmstadt, Germany) in accordance with the manufacturer's instructions. Cholesterol parameters were assessed using PPP samples as specified by the protocol. All measurements were finalized within 7 days of sample collection, with fresh PPP stored at 4°C.

3.8 Analysis of circulating EVs using flow cytometry

PFP samples stored at –80 °C were thawed and analysed on a CytoFLEX S N2-V3-B5-R3 Flow Cytometer (product # B78557, Beckman Coulter, Brea, USA). The measurements were performed using a "slow" flow rate setting of 10 µL/min over a 2-minute period, with events detected using a pre-optimized gate for EV detection, following protocols detailed in previous publications (64, 65). This setup incorporated the Flow Cytometry Sub-micron Particle Size Reference Kit (catalogue # F13839, Invitrogen, Carlsbad, USA) as shown in Figure 7.

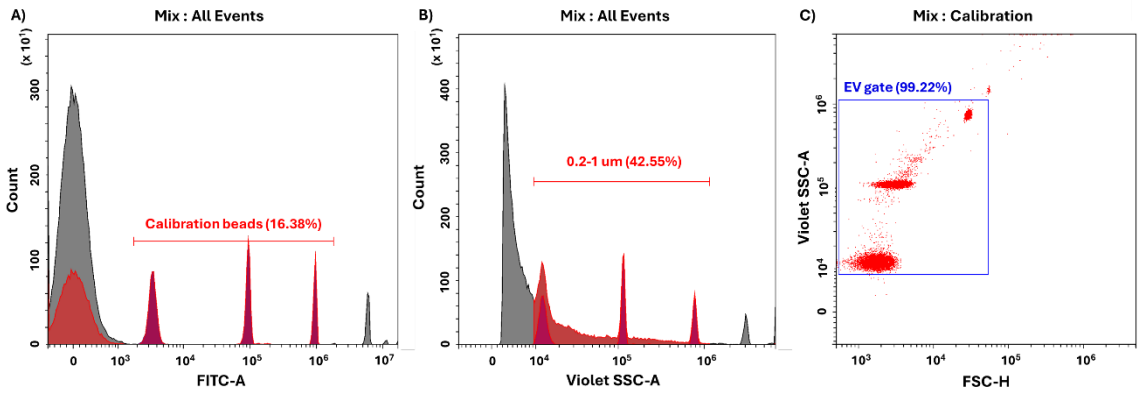

Figure 7. Three graphs above show the gating strategy used to set-up the EV gate in flow cytometry. **a** FITC-area/count graph showing all events displayed when reference size beads were measured by the instrument. The three sharp red peaks represent the beads of three different sizes (0.2, 0.5, and 1.0 µm) included in the kit. **b** A graph containing the Violet SSC-A/count. The three red peaks representing our three different sized beads mentioned above, as highlighted using the line segment. **c** FSC-hight /violetSSC-area used here shows the (forward/side) scatter of all events within the line segment seen in graph **a** within this figure. The proposed gate in blue, representing the EV gate. Figure adapted from supplementary data (61) of authors own first author publication.

Antibodies were diluted 10-fold in 0.1 µm filtered Annexin Binding Buffer (ABB: 10 mM HEPES, 140 mM NaCl, 0.25 mM CaCl2; pH 7.4–7.5) and centrifuged at 12,600 g for 10 minutes at 4°C. Carefully pipetted supernatants, ensuring no disturbance of antibody pellet aggregates, were transferred to new, labelled tubes. For mouse samples, 1 µL of PFP was used, and for human samples, 4 µL was used; these volumes were chosen after optimization testing with concentration curves used to avoid detector saturation while ensuring adequate particle counts, and without causing a swarm effect. Each sample was

prepared in a separate Eppendorf tube with antibody mixes ensuring no fluorescent overlap, these cocktails are specified in Table 2. Stained samples were protected from light and incubated at 4°C for 30 minutes. Following this, 30 µL of count check beads from Sysmex (Order # 05-4010, Lot KW190620, 37,920 particles/mL ±10%) was added to each sample, and ABB filtered at 0.1 µm was used to reach a final volume of 300 µL.

Table 2. Table two is divided into two main categories, the first of which is the mice antibodies used and the second is the human antibodies used. The second column is the target antibody use, column three is the provider of the antibody, column four is the catalogue number, column five is the conjugate used, and the sixth and final column shows the volume of each antibody used per sample. Table adapted from supplementary data of authors own first author publication (61).

Species	Antibody	Provider	Catalogue No.	Conjugate	Volume (µL)
Mice antibodies	Annexin V	Invitrogen	R37175	AlexaFlora647	7.2
	CD63	Sony Biotechnology	RT1319520	PE	1.8
	CD81	Sony Biotechnology	RT1124545	APC	1.2
	ApoB	Tresars	TR78654-02	FITC	1.5
	ApoE	Novus Biologicals	NB110-60531PCP	PerCP	N/A
	CD29	Sony Biotechnology	RT1111120	Pacific blue	1.5
	CD62P	Sony Biotechnology	RT1341520	APC	1.5
Human antibodies	Annexin V	Invitrogen	R37175	AlexaFlora647	7.2
	CD63	Sony Biotechnology	RT2365095	PerCP-Cy5.5	3.04
	CD81	Sony Biotechnology	RT2347575	Pacific blue	1
	ApoB	Tresars	TR78654-02	FITC	1.5
	ApoE	Novus Biologicals	NB110-60531PCP	PerCP	0.5
	CD29	Sony Biotechnology	RT2115040	APC	1.5
	CD62P	Sony Biotechnology	RT2124520	FITC	2

All flow cytometry data was processed with the CytExpert 2.1 software (Beckman Coulter, Brea, USA) and exported to Office365 Excel (Microsoft, Redmond, USA) for further analysis using the following formula.

$$\text{EV positive Events} = \left(\frac{\text{fluorescent events detected} - \text{staining background}}{\text{bead count}}\right) x \text{ bead concentration x} \left(\frac{\text{EV dilution}}{\text{bead dilution}}\right)$$

3.9 Bead-based analysis of clinical PFP lEVs

MACSPlex EV Kit IO, for human sample detection was used (catalogue # 130-122209, Miltenyi Biotec, Bergisch Gladbach, Germany) to evaluate EV associated markers from the PFP of clinical patients. Three patients from group A and from 3 patients from group

B (groups shown in Table 1) were measured. The MACSPlex EV Kit IO, mouse (catalogue # 130-122-211, Miltenyi Biotec, Bergisch Gladbach, Germany) was used for detection of above-mentioned markers in mice samples. Here, PFP samples were pooled from 6 animals from each group (WT, PCSK9, and LDLR) after HFD. Both the human and mouse samples were thawed from -80 ºC, and 1 mL from each human sample and 0.5 mL from pooled mouse samples were spun down at 20,000 g for 40 minutes using a refrigeration centrifuge, keeping samples at 4 ºC throughout the process. The supernatant of each sample was discarded, and pellets were each re-constituted in 100 µL PBS. As a wash step, samples were re-centrifuged using 20,000 g for 40 minutes at 4 ºC. Supernatants were carefully removed, and pellets were again re-constituted in 100 µL of PBS.

The total protein concentration of each processed sample was measured with the Micro BCA assay kit (catalogue # A55864 ThermoFisher, Waltham, Massachusetts, USA). Based on the Micro-BCA assay, 10 µg total protein was used from each sample to perform the MACSPlex measurement. The manufacturers protocol was followed here using steps for the overnight incubation. A sample containing only the MACSPlex kit's reaction buffer, their detection antibody cocktail mix, and capture beads was used as a negative control. The CytoFLEX S N2-V3-B5-R3 Flow Cytometer (product # B78557, Beckmann Coulter, Brea, California, USA) was used to measure all MACSPlex samples. All measurements were taken on medium speed setting at 30 µL/minute. The gating strategy used here, was based on the negative control sample and can be seen in Figure 8.

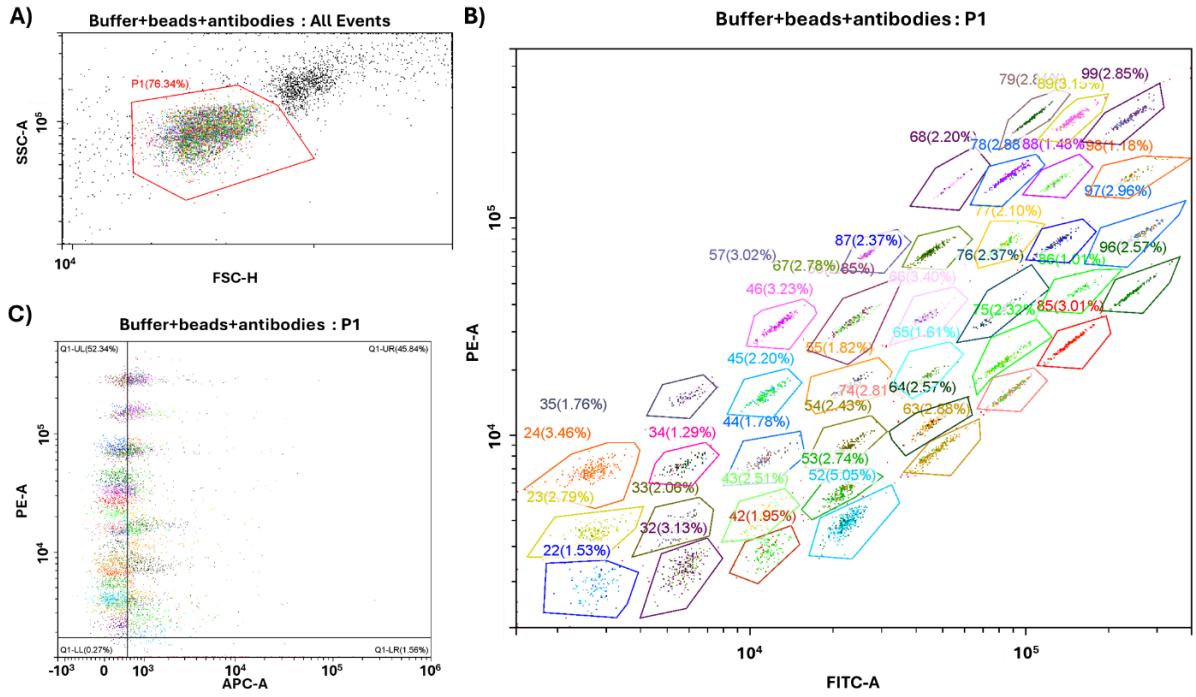

Figure 8. Three graphs display the flow cytometry set-up for the exosome (MACSPlex) capture beads. **a** FSC-hight/SSC-area was used to show the scatter of the overall bead population. **b** FITC-area/PE-area of the "P1" gate from graph **a** was used to display the 37 different sized beads (representing the 37 markers), each of which are gated in accordance with the manufacturer's layout. **c** The graph displays an APC-area threshold, for APC fluorescence using beads alone as a blank for which bound and stained exosomes will surpass. Figure adapted from supplementary data (61) of authors own first author publication

Each sample was processed by first subtracting the negative control signal from each marker, with any resulting negative values set to zero. The marker values were further adjusted by subtracting the highest isotype control signal for each sample. Averages were then calculated for each marker, followed by normalization to the mean of the standard EV markers (CD9, CD63, and CD81). The normalized data was subsequently plotted using GraphPad Prism 8.2.0.

3.10 Tissue culture

The isolation of human umbilical vein endothelial cells (HUVECs) was approved by the Ethical Committee Vote 200 (2005) from the State of Upper Austria. Thes HUVECs were

supplied to us from collaborators in at the Ludwig-Boltzmann-Institute for Traumatology in Vienna Austria. Frozen HUVECs were thawed from nitrogen storage and cultured in a tissue culture flask treated for cell adhesion, using endothelial cell growth media-2 (EGM2) supplemented with 10% fetal bovine serum until they reached 80% confluency. The cells were then detached with TrypLE™ Select Enzyme (catalog #12563011, Invitrogen, Carlsbad, USA), centrifuged at 200 g for 4 minutes, and resuspended in serum-free EGM2 after discarding the supernatant. Subsequently, the cells were seeded into a 6-well plate with each well containing 1 mL of serum-free EGM2. The cells were allowed to grow to 70% confluency before initiating the gene expression assay. At this stage, EGM2 media was removed, and each well was rinsed with PBS.

3.11 Isolation and quantification of lEVs

PFP was used from both normocholesterolaemic and hypercholesteraemic patients at a volume of 1 mL. PFP was thawed from -80 ºC and centrifuged for 40 minutes at 20,000 g and 4 ºC. Supernatants were discarded and resuspended in 100 µL EGM2 media and re-centrifuged for 40 minutes at 20,000 g and 4 ºC. The supernatant was once again discarded, and the pellets were reconstituted in 105 µL EGM2 media. From the resuspended pellets, 5 µL of each sample was used to quantify the EVs using nanoparticle tracking analysis (NTA), relying on Brownian motion for particle size and size distribution.

Particle size and concentration was measured using the ZetaView Z-NTA instrument from Particle Metrix (Munich, Germany). Samples were diluted either 1:250 (isolates from normocholesteraemic patients) or 1:2,000 (isolates from hypercholesteraemic patients) in PBS. Eleven positions were scanned across the flow cell, with duplicate measurements in each position as technical replicates. The instrument was maintained at a temperature of 25 °C to preserve a consistent Brownian motion. Measurements were achieved ensuring 150-300 particles in each position. The camera sensitivity was set to 75 using a shutter speed of 80 frame per second. The boundaries for analysis included: a maximum area: 1000, a minimum area: 5, excluding particle brightness < 20.

3.12 Gene expression assay

Based on particle concentration measured with NTA, 1.40E+09 lEVs were used per well in a 6-well plate for those conditions treated with lEVs. As a positive control, one well contained 10 µg/mL lipopolysaccharide (LPS), which was used to inducing inflammation. One well on the 6-well plate contained HUVECs and EGM2 media alone, for use as a negative control. Cells were incubated for 24-hours in an incubator at 37 ºC with 5 % CO_2 and 90 %–95 % humidity. After a 24-hour incubation, media was removed from wells, after which, all wells were washed with 1 mL PBS. PBS was removed and cells then suspended in 700 µgL of lysis reagent QIAzol (catalogue # 79306, Qiagen, Hilden, Germany). 140 µL of chloroform was mixed into each sample for phase separation and samples were centrifuged for 20 minutes at 20,000 g maintaining samples at 4 ºC throughout. The upper "clear" phase was carefully pipetted (ensuring no contamination from lower phases) onto columns from the GeneAid total RNA isolation kit (catalogue # RSD300, Geneaid, Biotech Ltd, New Taipei City, Taiwan) and steps from the kit's protocol for "clean-up", "washing" and "elution" of samples were followed. Figure 9 below shows a schematic outlining the key steps in the experiment design, showing the conditions of different wells allowing consequential mRNA changes in varying wells.

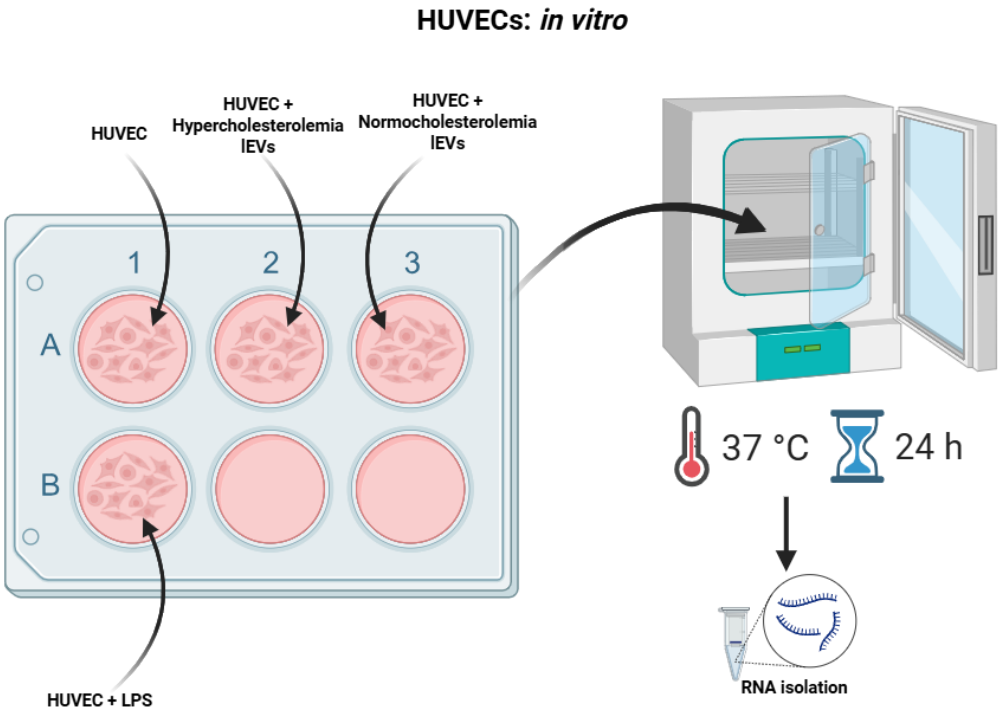

Figure 9. This diagram outlines the *in-vitro* work performed in this research. The diagram shows a 6-well plate with human umbilical vain endothelial cells (HUVECs), well-A1 is just HUVECs (negative control), well-A2 containing HUVECs with large extracellular vesicles (lEVs) isolated from plasma of hypercholesterolaemic patients, well-A3 containing HUVECs with lEVs isolated from plasma of normocholesterolaemic patients and well-B1 containing HUVECs treated with lipopolysaccharide (positive control). The plate was incubated for 24-hours at 37 ºC with 5 % humidity. After which, RNA was isolate from the HUVECs.

cDNA was synthesised from the RNA isolated with reverse transcriptase, using the SensiFAST cDNA kit (catalog # BIO-65054, Bioline, London, UK) according to the manufacturer's protocol. Quantitative PCR (qPCR) was then performed on the cDNA to assess gene expression in HUVECs incubated with lEVs isolated from normocholesterolemic and hypercholesterolemic patients, as well as HUVECs treated with LPS. All the CQ values were normalised to those obtained from cDNA of untreated HUVECs. TaqMan gene expression probes (catalog # 4331182, Applied Biosystems, Waltham, MA, USA) labelled with 6-carboxyfluorescein (blue)were used, and qPCR was conducted with 2× TaqMan™ Fast Advanced Master Mix (catalog # 4444557, Applied Biosystems, Waltham, MA, USA) per the manufacturer's instructions. Each well on the 384-well qPCR plate included an HPRT1 probe (catalog # 4448484, Applied Biosystems, Waltham, MA, USA) as a housekeeping gene control, the HPRT1 was labelled with a -2′-chloro-7′phenyl-1,4-dichloro-6-carboxy-fluorescein (green) .

Gene expression analysis covered several relevant genes including, CD36, CXCL1, HMOX1, IL6, PPARγ, TRIB1, and VEGFA across all experimental conditions. The BioRad CFX Opus 384 Real-Time PCR System (BioRad C1000 Touch Thermal Cycler, Hercules, CA, USA) was used here. Figure 10 is a brief schematic of the analysis of gene expression measurements performed in this project.

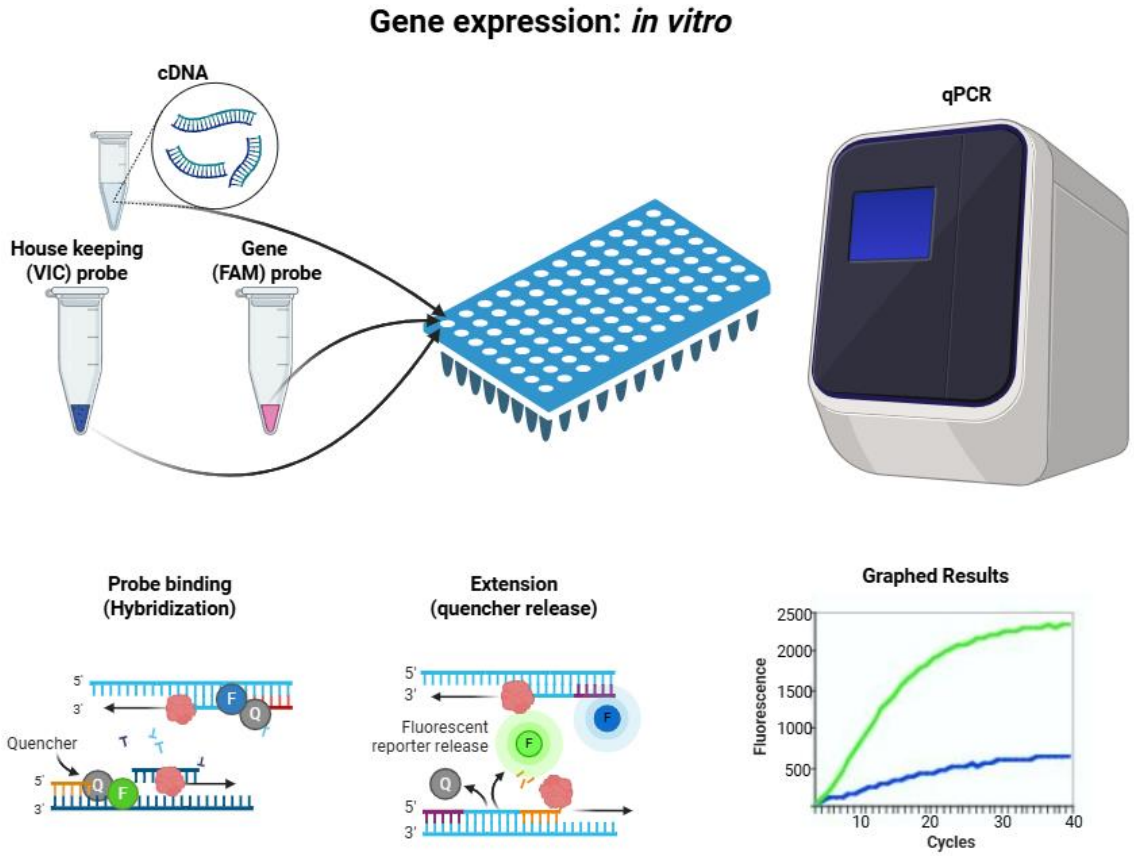

Figure 10. A schematic representation of the assessment of gene expression levels changes in HUVECs. cDNA from each biological condition was placed into a well on a 384-well plate alongside a genetic probe and a housekeeping gene probe. Using 2 probes per well, the qPCR amplifies both the gene of interest and the housekeeping. The difference in fluorescence between the housekeeping prob and gene of interest probe allows use of the housekeeping as a background control for each biological replicate. This allows more concise calculations of expression levels (with the use of ddCT value).

3.13 Statistical Analysis

GraphPad Prism version 8.2.0 (GraphPad Software, Inc.) was employed to perform all statistical analysis. All statistical data was performed using a 95 % confidence interval. Values are presented as means ± standard deviation with individually plotted points. The Shapiro-Wilk normality test was used to assess normality of all groups with a Gaussian distribution. In the Shapiro-Wilk normality test the null hypothesis is that the sample is normally distributed with p-value above 0.05 accepting this null hypothesis and considering the sample normally distributed while a p-value below 0.05 rejecting it and

indicating a non-normal distribution. For groups with normally distributed data, an unpaired student t test was performed and for groups that were not normally distributed, the non-parametric Mann-Whitney U test was used. For comparisons of data sets within a single group, a paired t test or a non-parametric Wilcoxon signed-rank test was selected depending on the normality of the samples.

4. Results:

4.1 Cholesterol levels and body mass of mice

Cholesterol levels and body mass of mice were measured from each mouse in all mice groups including WT, PCSK9$^{-/-}$, and LDL$^{-/-}$ mice. Measurements in all groups were taken at baseline, after HFD, and at old age. Figure 11 shows all the cholesterol measurements taken from all the mice at all the different time points with Figure 11**a** showing total cholesterol levels, Figure 11**b** showing LDL levels, and Figure 11**c** showing HDL levels. We also measured the body mass of all mice groups at the three given time points, the results can be seen in Figure 11**d**. As seen in the figure below (Figure 11**a**), TC levels are continuously significantly reduced in PCSK9$^{-/-}$ mice and raised significantly in LDLR$^{-/-}$. The same trend was observed in LDL levels (seen in Figure 11**b**). As seen in Figure 11**c,** HDL levels do not follow the same level of significance, but HDL levels do follow the similar trends of elevation and reduction that were observed in TC and LDL during HFD. The body mass of PCSK9$^{-/-}$ mice were significantly elevated compared to WT mice at all given time points.

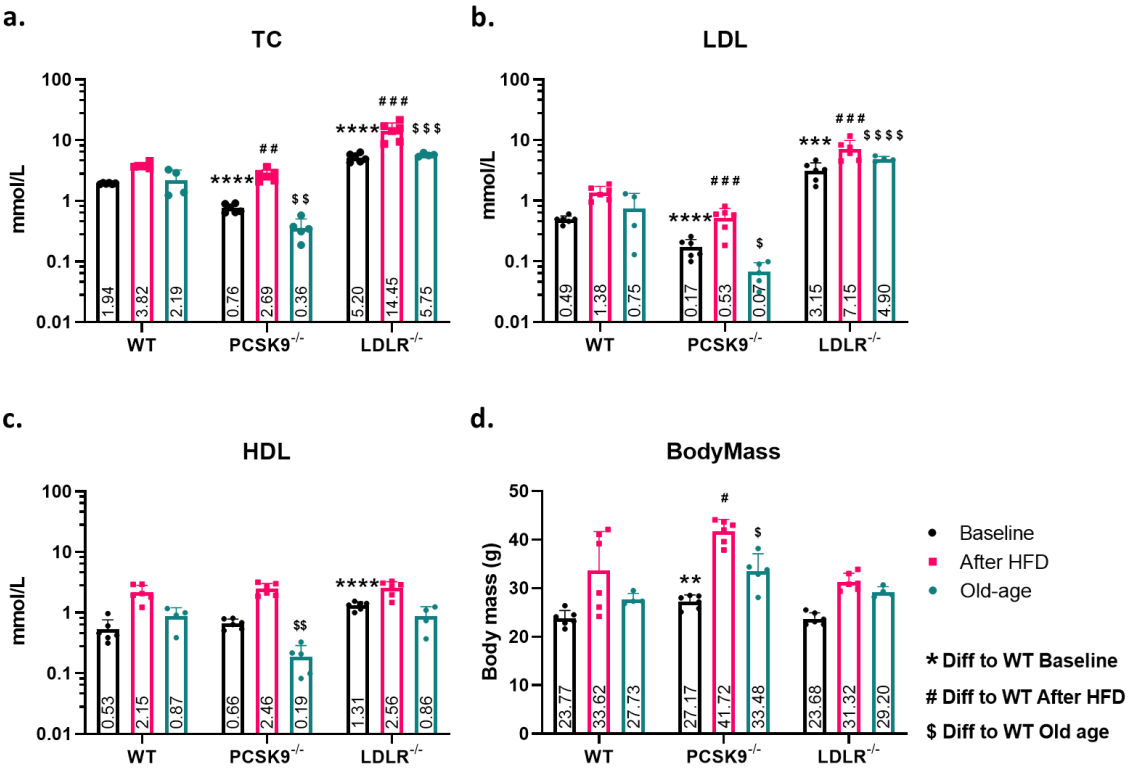

Figure 11. Cholesterol quantities in all mice as measured using a colorimetric assay. Measurements were taken at baseline, after high fat diet and in old age animals. Body mass was also assessed at these time points. **a** Total cholesterol (TC) levels in PCSK9$^{-/-}$ and LDLR$^{-/-}$ mice, compared to wild-type (WT) and a control. TC in PCSK9$^{-/-}$ mice were significantly lower than WT at all time points where LDLR$^{-/-}$ mice were elevated at all time points. **b** Low-density lipoprotein (LDL) levels in PCSK9$^{-/-}$ and LDLR$^{-/-}$ mice, using WT and a control. LDL levels were also depleted at al time points in PCSK9$^{-/-}$ mice at all time points, and elevated in LDLR$^{-/-}$ mice during all measurements. **c** High-density lipoprotein (HDL) levels in PCSK9$^{-/-}$ and LDLR$^{-/-}$ mice versus WT mice. HDL levels were significantly reduced in PCSK9$^{-/-}$ mice at old age and significantly elevated in LDLR$^{-/-}$ mice at baseline when compared with WT group. **d** Body mass levels of all three mice groups at all three time points. PCSK9$^{-/-}$ levels were significantly elevated at all three time points compared to WT mice, with LDLR$^{-/-}$ showing no changes. One, two, three, or four (*), (#), or ($) represent repectively $p < 0.05$, $p < 0.02$, $p < 0.002$, or $p < 0.0001$. Figure adapted from authors own first author publication (61).

4.2 Cardiovascular parameters and atherosclerosis quantification in mice

A major motivation for this study was to investigate not only the circulating EV levels in comparison to the cholesterol, but more directly to link the EV levels to atherosclerosis and the development of ischemic cardiovascular disease. For this reason, we assessed cardiovascular function and additionally evaluated the plaque levels in all mice. Figure 12 a-d shows cardiovascular function measured using ultrasound and aortic arch plaque levels using Oil-Red-O staining. Figure 12 shows data of mice at baseline as well as those after HFD, with graph a representing ejection fraction, b showing cardiac output, c displaying fractional shortening, and d representing E/é ratio.

Figure 12e shows representative images of stained aortic arches after HFD, as well as a graph displaying percentage area of plaques as measure at baseline and after HFD. Figure 13 shows data of mice at baseline as well as at old age. Here like Figure 13, graph a signifies ejection fraction, b showing cardiac output, c displaying fractional shortening, and d representing E/é ratio. Figure 13e shows a representative image from each mouse model of stained aortic arches after at old age, with a graph exhibiting percentage area of plaques as measure at baseline and at old age. In the study we also measured

cardiovascular wall thickness at several key junctions. Graphs in Figure 14 show the LVPW;d and the LVAW;d as measure at baseline (Figure 14a), after HFD (Figure 14b) and at old age (Figure 14c).

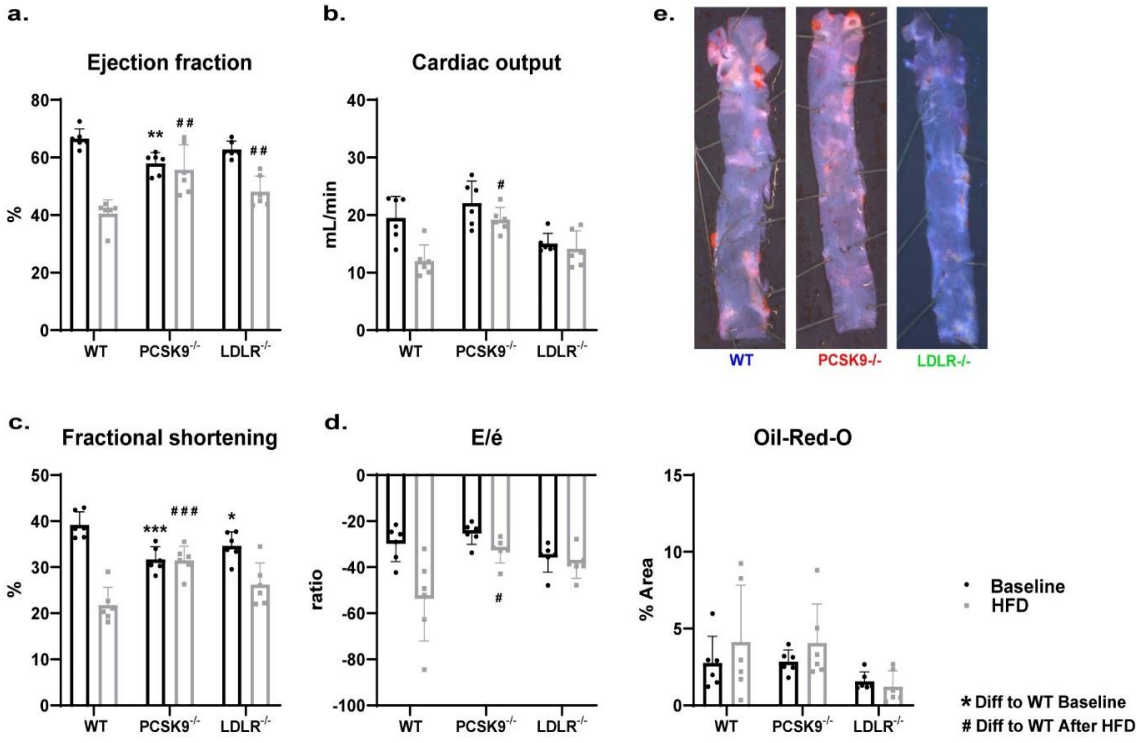

Figure 12. Cardiovascular parameters and atherosclerosis measured in all three mice groups, as seen at baseline and after high-fat diet (HFD) for all mice. **a** Ejection fraction readings of all mice. After HFD both PCSK9$^{-/-}$ and LDLR$^{-/-}$ were significantly elevated. **b** mL of blood circulated per minute given as cardiovascular output. PCSK9$^{-/-}$ animals show significant improvement over wild type (WT) after HFD. **c** measurements of fractional shortening of the left ventricle during systole in all mice. After HFD, compared to WT mice, fractional shortening is significantly elevated in the PCSK9$^{-/-}$ mice. **d** Measurements of early diastolic mitral inflow velocity to early diastolic mitral annulus velocity (E/e') ratio, estimating the left ventricle filling pressure. PCSK9$^{-/-}$ mice show a significantly less negative E/e' ratio compared to WT. **e** Representative images of Oil-Red-O stained aortic arches from each mouse model estimating plaque levels, and a graph showing percentage area of staining on each aortic arch of individual mice. No significant changes were observed after HFD between mice groups. One, two, three, or four (*), or (#), represent repectively $p < 0.05$, $p < 0.02$, $p < 0.002$, or $p < 0.0001$. Figure adapted from authors own first author publication (61).

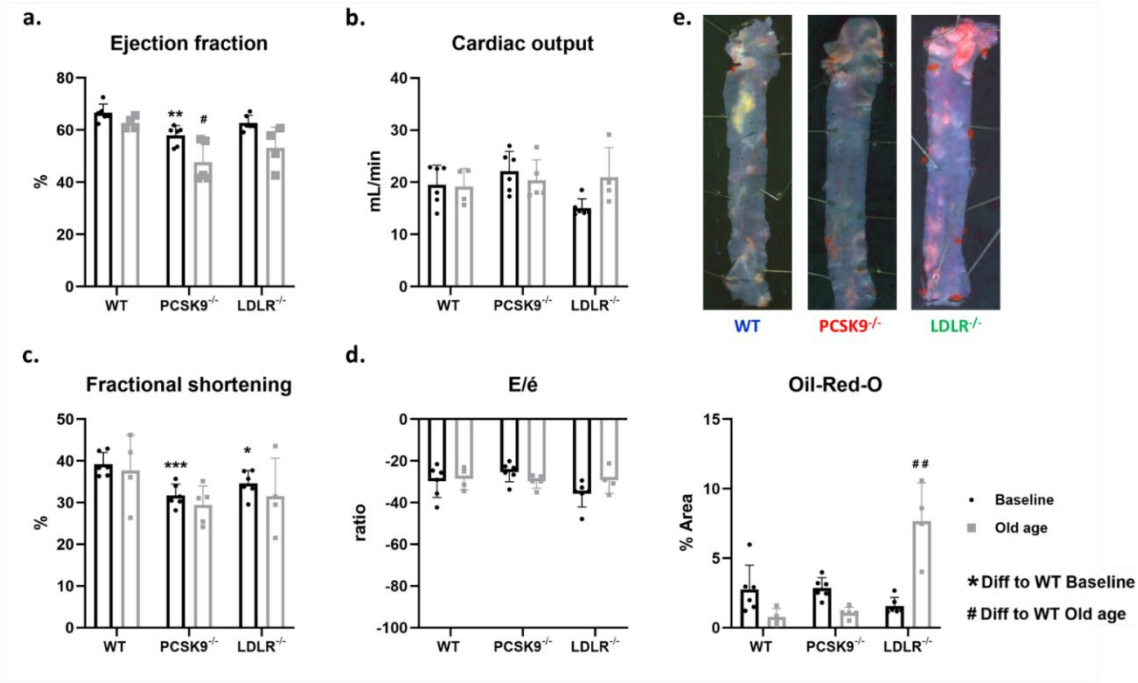

Figure 13. Cardiovascular parameters and atherosclerosis measured in all three mice groups, as seen at baseline and at old age for all mice. **a** Ejection fraction readings of all mice. **b** mL of blood circulated per minute given as cardiovascular output. **c** measurements of fractional shortening of the left ventricle during systole in all mice. **d** Measurements of early diastolic mitral inflow velocity to early diastolic mitral annulus velocity (E/e') ratio, estimating the left ventricle filling pressure. No significant alterations were observed between groups in old age animals in regard to cardiovascular parameters (**a-d**) measured above. **e** A representative image of Oil-Red-O stained aortic arches from each mouse model estimating plaque levels, and a graph showing percentage area of staining on each aortic arch of individual mice. A significant level of plaque was observed in LDLR$^{-/-}$ mice in old age compared to their wild type equivalents. One, two, three, or four (*), or (#), represent repectively $p < 0.05$, $p < 0.02$, $p < 0.002$, or $p < 0.0001$. Figure adapted from authors own first author publication (61).

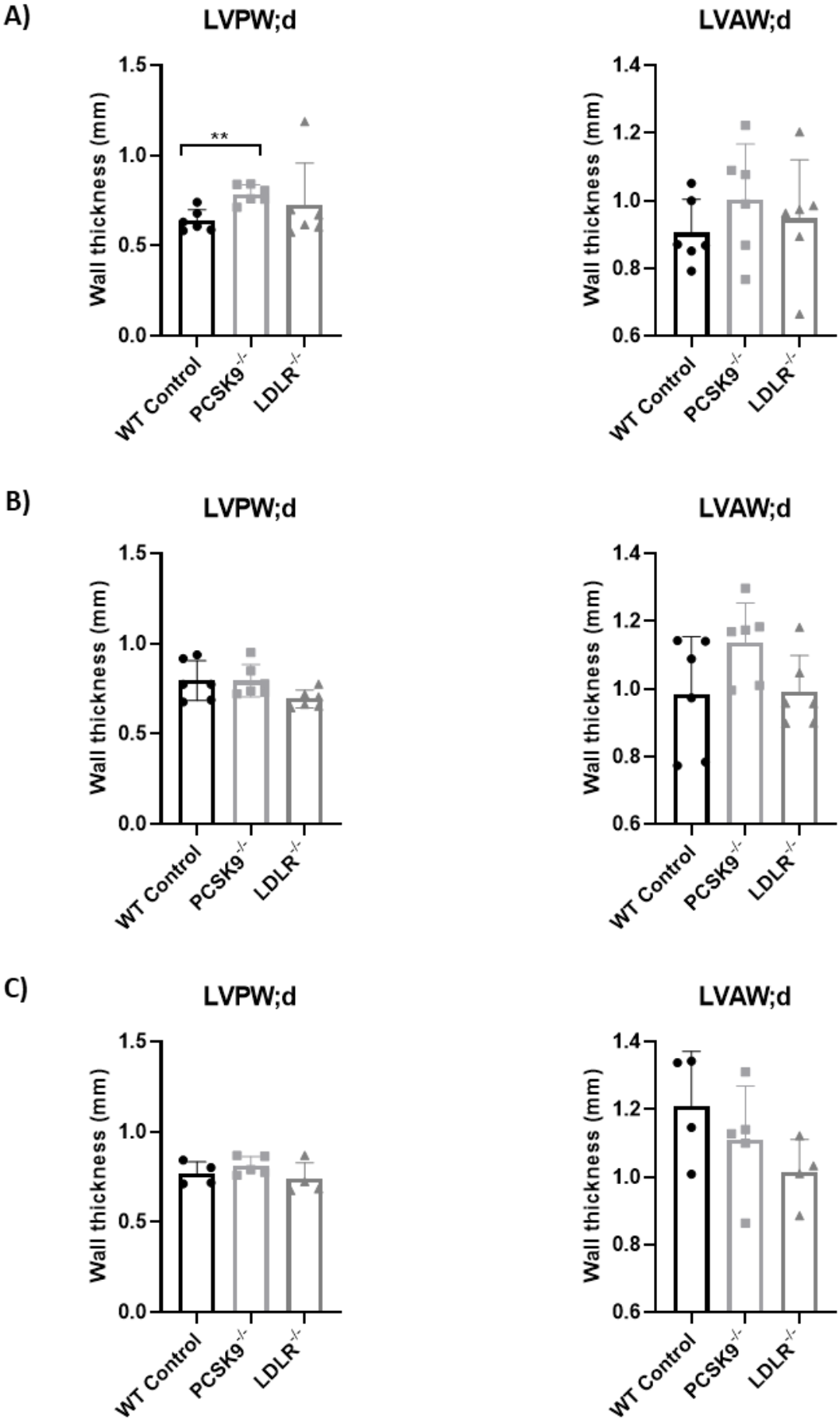
A)
LVPW;d
LVAW;d
Wall thickness (mm)
1.5
1.0
0.5
0.0
1.4
1.2
1.0
0.8
0.6
**
WT Control
PCSK9-/-
LDLR-/-
B)
LVPW;d
LVAW;d
C)
LVPW;d
LVAW;d

Figure 14. Measurement of cardiovascular wall thickness at three different time point. Measurements were taken at baseline, after high-fat diet (HFD) and at old age. Measurements are estimated using Doppler technology during the echo examination, with estimated left ventricle posterior wall thickness (LVPW;d) and left ventricle anterior wall thickness (LVAW;d) being assessed. **a** LVPW;d and LVAW;d measurements for mice at baseline. A significant increase in LVPW;d was observed in baseline PCSK9$^{-/-}$ compared to wild type mice . **b** measurements of LVPW;d and LVAW;d of all mice after HFD. **c** LVPW;d and LVAW;d as estimated in all mice at old age. One, two, three, or four (*), (#), or ($) represent repectively $p < 0.05$, $p < 0.02$, $p < 0.002$, or $p < 0.0001$. Figure adapted supplementary data from authors own first author publication (61).

4.3 Circulating lEV levels and lEV sized ApoB levels in mice

Flow cytometry was used to assess lEV levels in PFP of all mice at baseline, after HFD, and at old age. PFP was also labelled with ApoB to assess levels of similarly sized lipoproteins in the same preps of PFP. Figure 15 shows levels in each group (WT, PCSK9$^{-/-}$, and LDLR$^{-/-}$) separately, where significance can be observed between groups at varying time points (baseline, after HFD, and at old age). Figure 15a shows annexin V labelled lEVs measured in all mice groups at the three above mentioned time points. Figure 15b shows measured levels of CD63, Figure 15c displays measured CD81 levels in all mice, and Figure 15d shows ApoB levels at all time points in all mice. Figure 16 displays graphs of the lEVs as well as comparable sized ApoB reading, with all groups merged (WT, PCSK9$^{-/-}$, and LDLR$^{-/-}$), highlighting the change observed after HFD or at old age (compared to baseline).

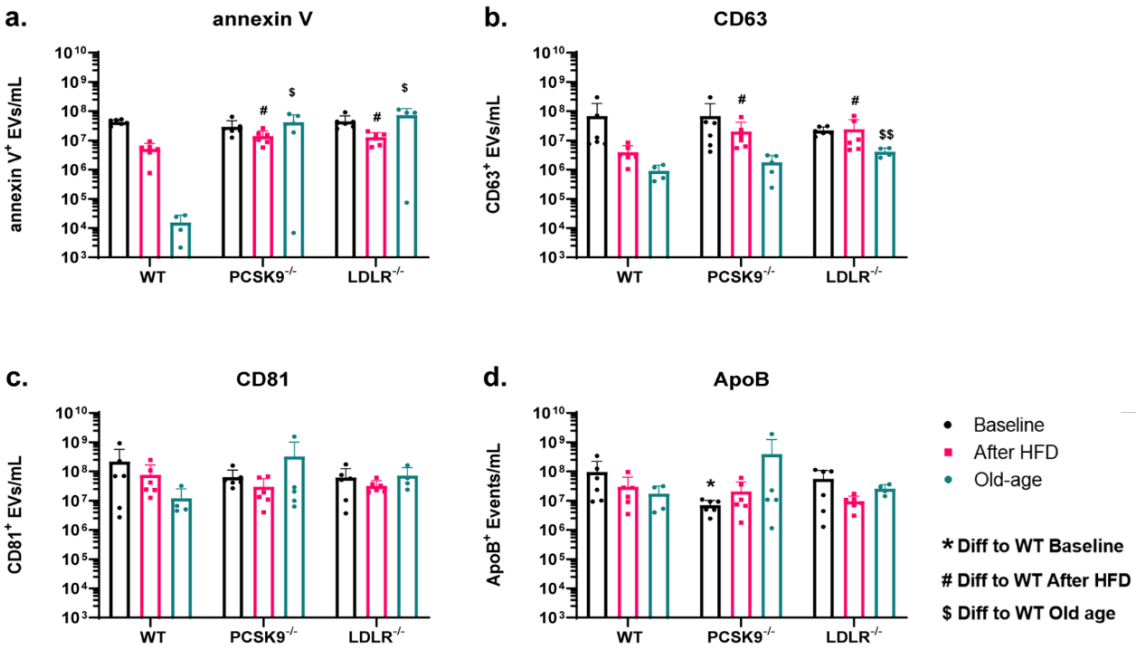

Figure 15. Single EV levels measured using flow cytometry, applying classic EV markers. Platelet free blood samples from each mouse within each group was measured at baseline, after high fat diet (HFD), and at old age. For EV measurements, annexin V and two classic EV Tetraspanin markers (CD63 and CD81) were measured. Apolipoprotein-B (ApoB) levels were also assessed. **a** Annexin V measured at all time points for all groups. PCSK9$^{-/-}$ and LDLR$^{-/-}$ mice both had an increase compared to wild type (WT) after HFD and at old age. **b** A graph showing CD63 measurements for all mice. PCSK9$^{-/-}$ and LDLR$^{-/-}$ mice both had an increase compared to WT after HFD and LDLR$^{-/-}$ show an increase level at old age. **c** CD81 levels shown in all mice at all time points. No significant differences were observed between groups. **d** ApoB levels measured in all mice at the three above mentioned time points. As seen in the graph, PCSK9$^{-/-}$ had a significantly lower ApoB level at baseline compared to WT animals. One, two, three, or four (*), (#), or ($) represent repectively $p < 0.05$, $p < 0.02$, $p < 0.002$, or $p < 0.0001$. Figure adapted from authors own first author publication (61).

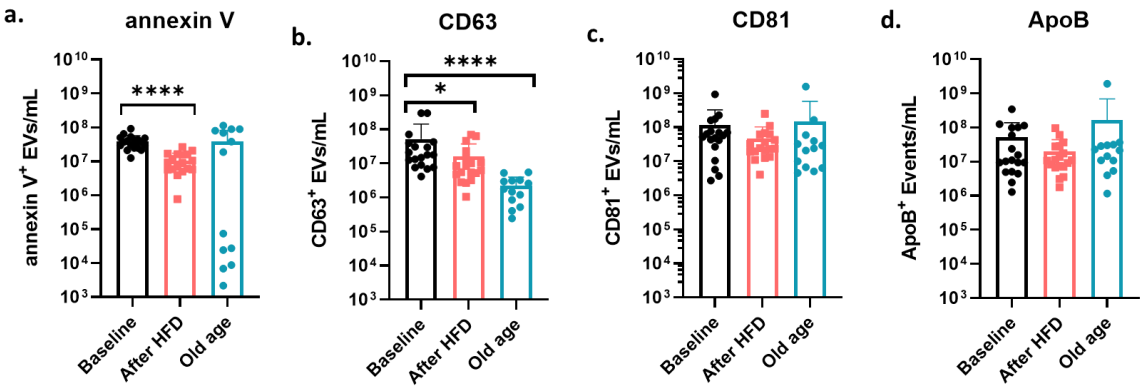

Figure 16. All mice models are displayed together, here the difference between EV and EV sized apolipoprotein particles can be observed in high fat diet (HFD) and old age, compared to wild type (WT) mice. **a** A graph showing annexin V measurements at three timepoints. As seen a significant reduction of lEV levels after HFD was observed. **b** Here CD63 levels can be observed, and as shown, levels of CD63 are significantly reduced after HFD and at old age compared to baseline levels. **c** The graph here shows CD81 levels and as seen, no significant changes are observed. **d** ApoB levels are shown in the graph. Here too, no significant changes were observed. * $p < 0.05$, ** $p < 0.02$, *** $p < 0.002$, and **** $p < 0.0001$. Figure adapted from authors own first author publication (61).

4.4 Circulating cholesterol and lEV levels in prandial and fasting mice

To further evaluate the association between cholesterol and EVs, it was decided to measure EV levels as well as cholesterol levels without fasting the animals (prandial measurement), where circulating cholesterol is often elevated. In Figure 17a cholesterol levels can be observed, as seen, TC and HDL levels are significantly reduced when animals are fasted for 5 hours. Figure 17b shows lEV levels from prandial and fasted mice, with no significant changes observed.

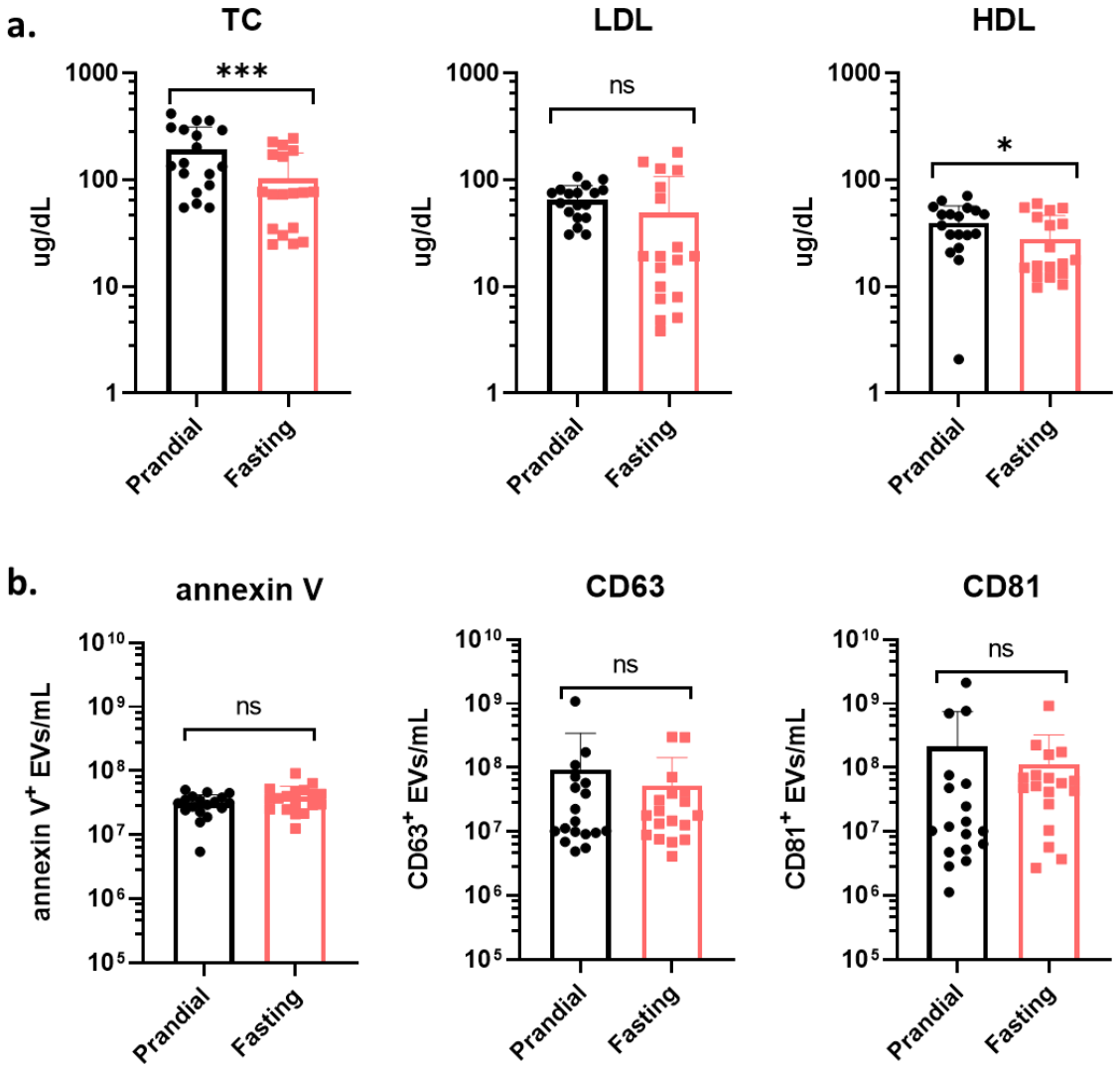

Figure 17. Prandial biomarker levels were also measured. Here prandial versus fasting were plotted against each other to observe changes in prandial blood. **a** Three graphs displaying prandial versus fasting cholesterol levels, with total cholesterol and high-density lipoprotein levels shown to be significantly altered. Low-density lipoprotein levels show no significant differences. **b** Three graphs showing annexin V, CD63, and CD81 levels respectively, no significant differences between the two time points were observed using any of these EV markers. * $p < 0.05$, ** $p < 0.02$, *** $p < 0.002$, and **** $p < 0.0001$. Figure adapted from authors own first author publication (61).

4.5 Circulating cholesterol, lipoprotein and lEV levels in normocholesterolaemic and hypercholesterolaemic patients

We needed to find out whether the findings in mice were translatable to clinics. We took PFP samples from clinic of patients suffering acute angina. The clinic measured the levels of cholesterol in all patients. We divided these patients into two groups. Those with normal TC levels and those with high levels of TC. Figure 18a shows the levels of TC, LDL, and HDL in each group. As with mice samples Apolipoprotein associated with lEVs are of interest here. Figure 18b shows the levels of lEV sized ApoB and ApoE measured in the clinical samples in either group. Finally, Figure 18c shows lEV levels as measured using flow cytometry.

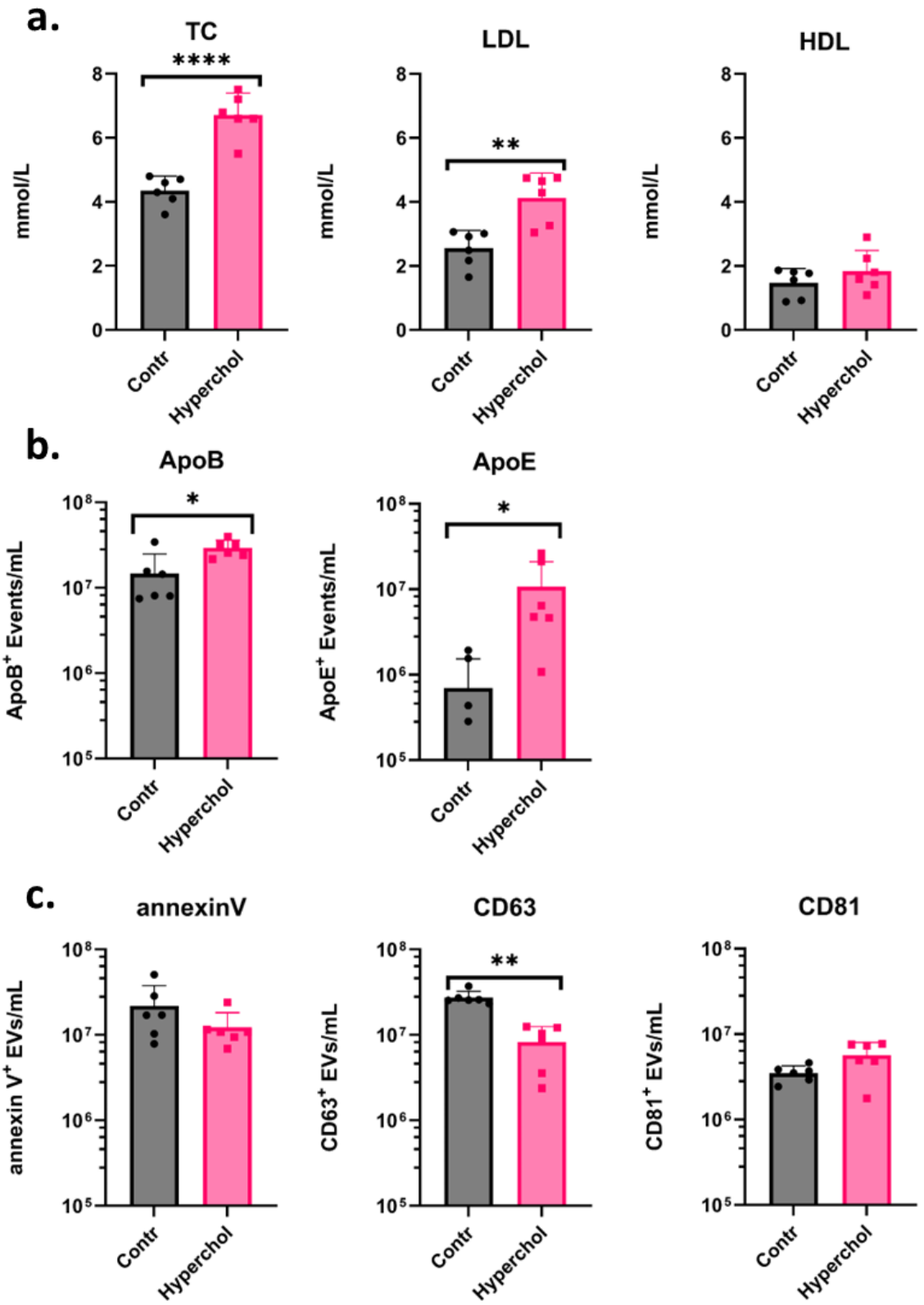

Figure 18. Cholesterol levels, large extracellular vesicles (lEV) sized apolipoprotein (Apo) levels, and lEV sized EV marker levels in hypercholesterolaemia versus control patient. **a** Graphs showing the hypercholesterolaemia versus control patient levels of total

cholesterol (TC), low-density lipoproteins (LDL), and high-density lipoproteins (HDL). The hypercholesterolaemia group show significantly elevated TC and LDL levels, while HDL levels remained unchanged between groups. **b** Two graphs showing lEV sized particles stained for ApoB and ApoE. Here, both ApoB and ApoE levels are significantly elevated with hypocholesterolaemia. **c** Three graphs show lEV levels as stained with classical EV markers. CD63 levels are significantly reduced in hypercholesterolaemic patients, while annexin V and CD81 show no changes. * $p < 0.05$, ** $p < 0.02$, *** $p < 0.002$, and **** $p < 0.0001$. Figure adapted from authors own first author publication (61).

4.6 Qualification and quantification of other EV markers found in mouse and human PFP

After our assessment of single EVs, we sought to identify other possible EV subpopulations and allow identification of likely cell of origin of our EVs. Here, we employed the MACSplex bead-based exosome kits to identify an array of EV markers and markers of cell involved in typically found in circulation. The kits used allow for measurement of 37 markers. In Figure 19a the top 10 most abundant biomarkers from the measurements in mice samples are displayed, alongside the three conventional EV Tetraspanin markers (CD9, CD63, and CD81). In Figure 19b the top 10 most abundant biomarkers from human samples measured are displayed, together with the three conventional EV Tetraspanin markers (CD9, CD63, and CD81). Markers CD29, CD31, CD49e, and CD62P are shown to elevated in both mice and human exosome capture, using the present array. Other markers found in relative abundance in mice samples include CD41, CD44, CD49b, CD61, and CD66a. Other markers amongst the top 10 most abundant markers in human samples include: CD24, CD40, CD41b, CD42a, HLA-ABC, and HLA-DRDPDQ.

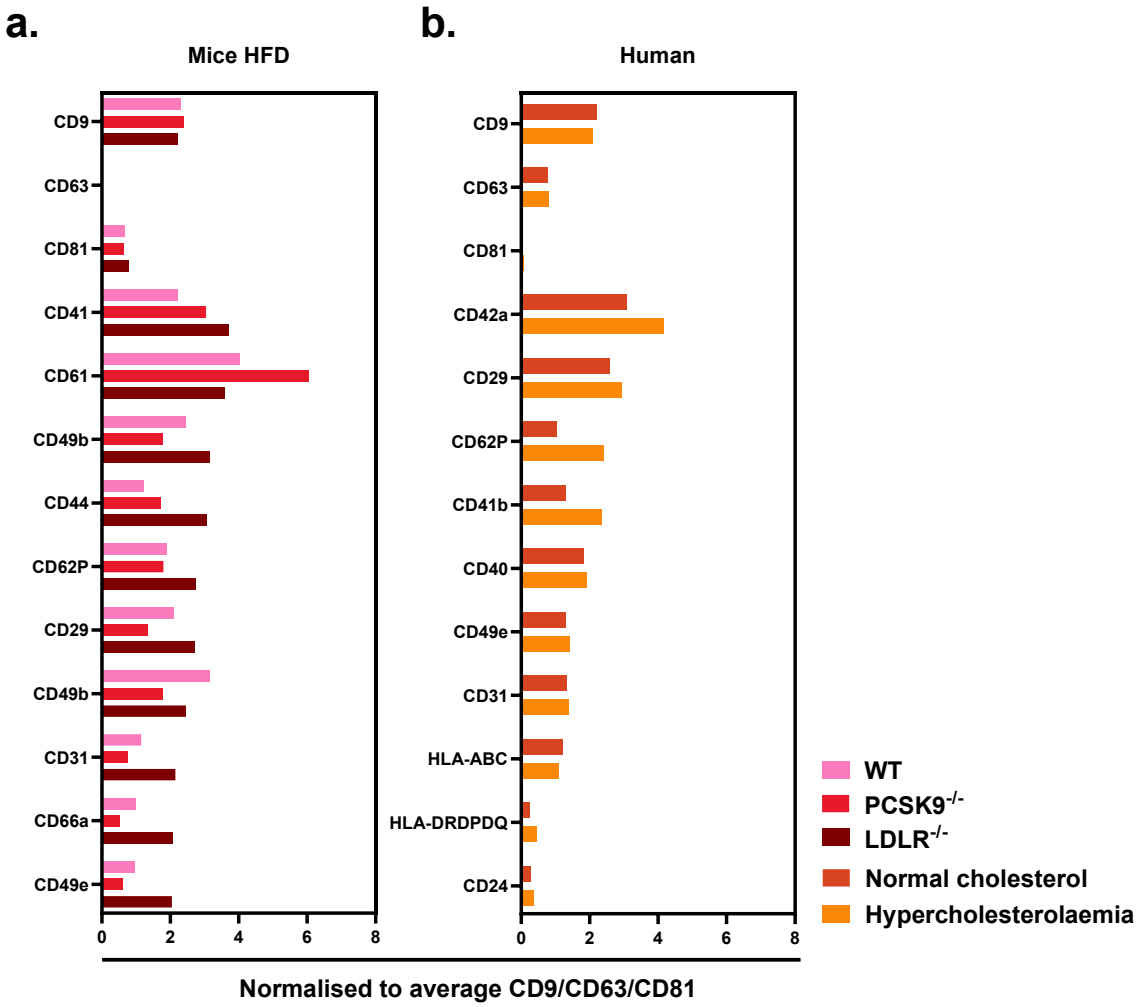

Figure 19. Exosome bead based kit used to test an array of known exosome surface markers from blood. Platelet free plasma (PFP) samples were used to assess exosome levels found in PFP and the cell source of those exosomes. In the figure, the three common extracellular vesicle Tetraspanin markers (CD9, CD63 and CD81) as well as the top 10 most abundant exosome markers found are presented. Levels are presented as a mean of three samples in each group. **a** Marker levels presented as they are found in the three mouse models used in this study. **b** Marker levels shown as they were found in the two cholesterolaemic human groups used in this study. Figure adapted from authors own first author publication (61).

Based on the results seen with the use of the MACSplex bead-based exosome kit, we wanted to see if some other abundantly available markers which were highlighted using the kit also had significant alterations between cholesterolaemia groups in both mice and human. Markers CD29 and CD62P were selected due to the abundance in both mice and

human samples, as well as their seeming corelation to cholesterol levels. Figure 20a shows the levels of CD29 and CD62P as measured using single EV detection techniques. In Figure 20b we show the levels of CD29 as well as CD62P levels measured using cytometry of single EV.

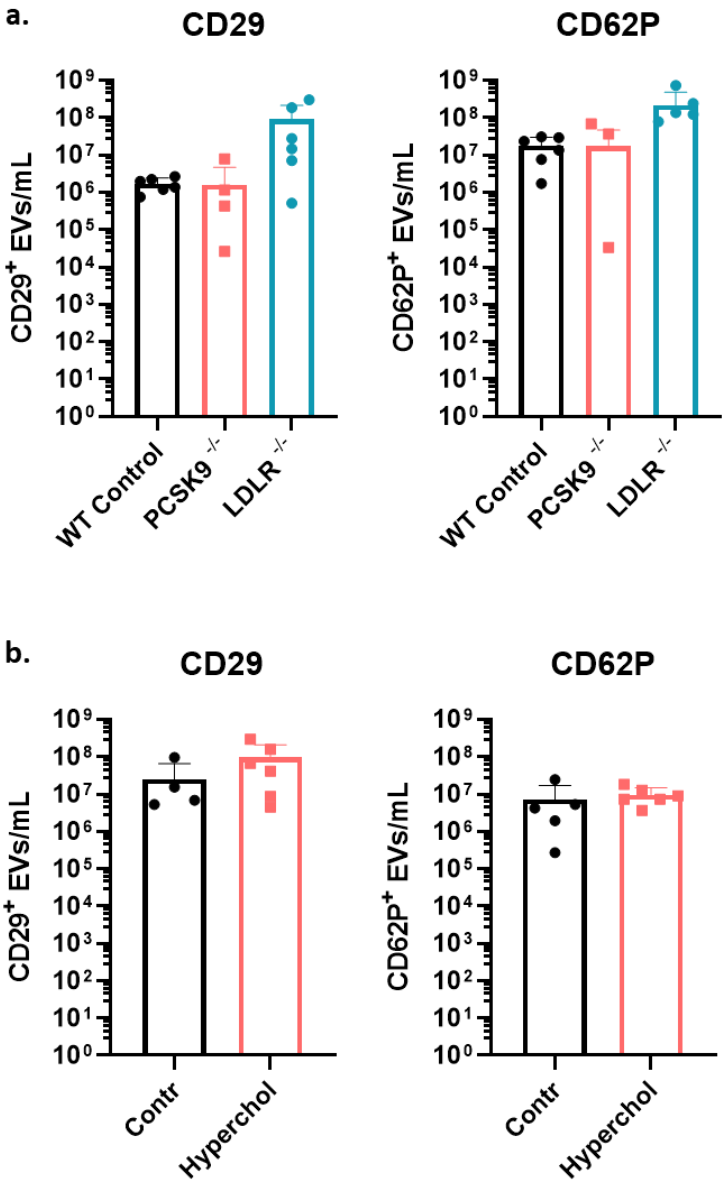

Figure 20. CD29 and CD62P levels were assessed here using flow cytometry and antibody staining. Gating's were set based on large extracellular vesicles **a** Measurements were performed on mice platelet free plasma (PFP) from blood taken after high fat diet. No significant differences were observed between any mouse group using either marker. **b** Two graphs show CD29 and CD62P levels in human PFP from hypercholesterolaemia

patients versus normocholesterolaemic patients. As seen in both graphs, no significance was found between CD29 or CD62P levels both *in-vivo* or in clinical groups. Figure adapted from supplementary data from authors own first author publication (61).

4.7 Gene expression of HUVECs after incubation with EVs isolated from cholesterolaemia patients

The earlier results of changes to EVs in circulation in hypercholesterolaemia insinuated an involvement of EVs in atherosclerosis. This led us to question the potential of these EVs as a cause in inflammation. Figure 21 shows the gene expression as a fold change compared to normalised data obtained from untreated HUVECs normalised to 1. The graph shows a panel of 7 markers involved in inflammation and CVD. Here LPS was used as a positive control and each data point was normalised to an internal housekeeping (HPRT) gene.

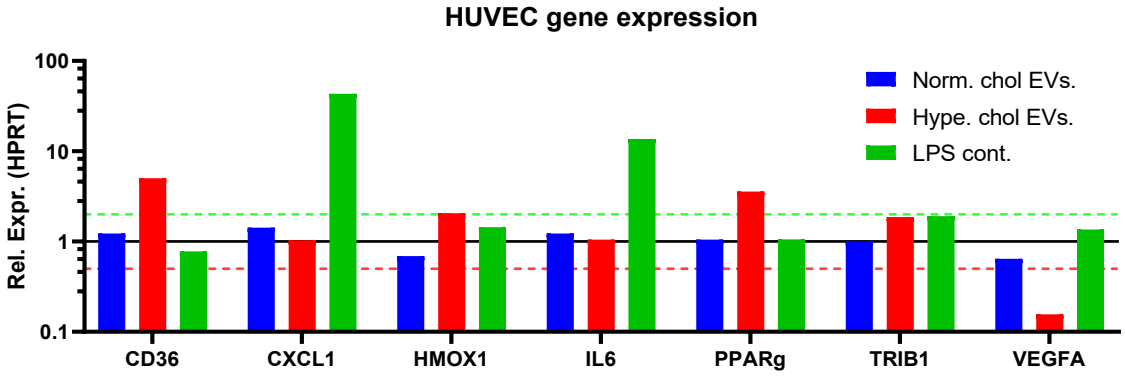

Figure 21. The above figure shows a graph containing gene expression data from HUVECs incubated with either large extracellular vesicles (lEVs) from patients with normal cholesterol levels or lEVs isolated from patients with hypercholesterolaemia. Lipopolysaccharide (LPS) was used as a positive control for inflammation. Gene expression levels are indicated as relative expression levels to internal housekeeping gene HPRT1, and all data was normalised to expression levels of HUVECs alone (negative control). Data points above 2 fold (green dotted line) expression is considered notably elevated and expression levels below 0.5 fold (red dotted line) negative control, are considered prominently reduced. CD36, HMOX1, and PPARg were shown to be elevated in HUVECs incubated with lEVs from hypercholesterolaemic patients, while VEGFA expression was low in these HUVECs. HUVECs incubated with lEVs from

normocholesterolaemic patients were unchanged in all tested genes. Here $n = 1$. Figure adapted from supplementary data of authors own first author publication (61).

5. Discussion:

Cholesterol levels, particularly LDL-C, are widely recognized as key biomarkers in assessing the risk and progression of ACVD (66). Our findings indicate that HFD contributes to an elevated LDL-C level at least in the mouse models examined here. In contrast, lower LDL levels were observed in younger mice at baseline as well as levels observed in older mice, both without HFD exposure. This finding suggests that concerning cholesterol dysregulation at least, diet can still be considered a strong contributor. With regards to atherosclerosis and more generally considering CVD, HFD as a contributing factor can still be debated. Genetically, we observed that compared to WT animals, at all-time points in the study, $PCSK9^{-/-}$ and $LDLR^{-/-}$ mice showed contrasting effects with regards to both LDL-C and total cholesterol (TC) levels. With $PCSK9^{-/-}$ mice showing lower cholesterol, and $LDLR^{-/-}$ mice a consistent increase relative to WT animals.

Although following HFD increased TC and LDL-C levels were observed, the genetic background of the mice emerged as a more influential factor in determining cholesterol levels. This is shown by the particularly elevated cholesterol in $LDLR^{-/-}$ mice. Interestingly, HDL-C levels, often referred to as "good cholesterol," (67) also increase in response to HFD. Likewise, HDL readings in $LDLR^{-/-}$ mice showed a highly significant increase over the WT mice at even in young animals before HFD commencement. As a rule, our data seems to indicate that HDL levels are typically altered following direct proportionality to other classes of "bad cholesterol" cholesterol. As is already known, HDL is key in cholesterol clearance from peripheral tissue including arteries, thus reducing LDL, VLDL, and Chylomicrons (including other intermediaries) from circulation. This happens due to the transfer of cholesterol from lipoproteins with lover densities to HDL via transport proteins ABCA1 and ABCG1. In this manner cholesterol can subsequently be reverse transported to the liver via hepatic – HDL complex for storage or later degradation in bile.

Our results may therefore suggest that perhaps in the absence of the LDLR gene (which typically acts as a primary LDL regulator), HDL production is increased to take a more prominent role in this process of cholesterol regulation thereby aiding in maintaining circulating cholesterol homeostasis. Recent studies have also indicated that higher

circulating HDL levels may in reality not be as favourable as previously thought (68, 69), perhaps making the increased HDL levels seen here an additional contributing factor to the ever growing instability in dyslipidaemia. Nonetheless, it is important to mention that what is considered healthy levels of lipids, cholesterol, and lipoproteins in mice differs quite substantially when compared to humans (70) and indeed often differ from species to species. For this reason, although the data here can be used to better understand the biological processes involving cholesterol and lipoprotein dysfunction, a more comprehensive studies would be helpful for any clinical applications.

Our data also highlighted an increase in body mass and visceral fat in PCSK9$^{-/-}$ mice, consistent with previous work (71) from other researchers. This phenomenon was initially difficult to comprehend, given the stereotype of high cholesterol observations in those with increased visceral fatty tissue. Although this has not been the narrative for some time, the initial observation of a complete inverse of this occurrence in a PCSK9$^{-/-}$ model was somewhat surprising to us. Aside from LDLR regulation and degradation, the PCSK9 gene serves many other functions in body, and exploration of this gene and associated proteins are still a hot topic, with most interested in its therapeutic applications in ACVD (55, 72). This also means that disruption of normal PCSK9 function may also lead to other health detriments (73). One such example of this, is that PCSK9 is a regulator of the B-scavenger receptor CD36. In the present research, the deficiency of PCSK9 in the PCSK9$^{-/-}$ model we investigated, aside from the expected elevated LDLR presence, CD36 expression may be highly elevated as well. CD36 in turn is highly involved in the transport of triglycerides as well as long-chain fatty acids (74). With lower levels, or indeed in the absence of PCSK9, excess CD36 accumulation is perhaps but one explanation for lipids accretion in various tissues (74, 75).

This work also shows that following a 12 week HFD, PCSK9$^{-/-}$ mice largely retained cardiovascular function, showing increased ejection fraction, cardiac output, fractional shortening, and a more favourable E/e' ratio compared to their WT counterparts. This goes in line with theories of a cardioprotective role for PCSK9 suppression under high-cholesterol conditions, supporting not only the narrative of cholesterol as key player in vascular diseases, but also supports the therapeutic use of PCSK9 inhibitors like alirocumab (Praluent) and evolocumab (Repatha) in hypercholesterolemia treatment. Nonetheless, the association of PCSK9 inhibition with increased body mass in mice, and

as it has also been observed in patients with PCSK9 mutations (71), raises important questions about the potential long-term effects of PCSK9 gene editing on patients. Concerns of such treatment therefore need further evaluation as to what this could possibly indicate with regards to both physical health and well-being, as well as the mental health (71, 76, 77) of treatment recipients.

Since ACVD is the leading cause of CVD, evaluating atherosclerotic plaque burden may provide a more significant measure of cardiovascular health. In mice, arterial plaque formation most frequently occurs in the aortic root (63). We therefore chose to analyse atherosclerotic plaque accumulation on the aortic arch in mice groups, allowing us to compare the risk of arterial blockages in these cholesterol-altered models. Our findings showed no significant differences between PCSK9$^{-/-}$, LDLR$^{-/-}$, and WT mice at baseline or after an HFD. With an average lifespan of roughly 18 months to 2 years, C57BL/6 background mice serve as an effective model for age-related research. (78). As with many pathologies, in an aging population, CVD risk surges (3, 79). Consequently, we included an old-age condition in our study. What we observed is that older mice the LDLR$^{-/-}$ group showed a significant increase in plaque formation compared to aged WT mice. This finding suggests that, within the short-term 12-week period mentioned earlier, HFD may have less impact on plaque formation than prolonged exposure to high cholesterol levels as observed in older LDLR$^{-/-}$ mice.

These results may more accurately reflect patterns seen in clinical studies of hypercholesterolaemia and aging (3). Considering that at baseline and in old-age, cholesterol levels are similar within each genetic group, and that WT and PCSK9$^{-/-}$ mice have normal or low cholesterol, in contrast to the higher levels seen in LDLR$^{-/-}$ mice, this may explain why plaque levels are significantly lower in the former groups at old age. This also highlights the slow development of atherosclerosis, and as other research shows, that ACVD only occurs after long exposure to harmful substances causing vascular damage, and eventually allowing plaque formation (80, 81).

A major motive for this study was to explore the relationship between EV levels and lipoproteins, particularly lEVs and LDL, using flow cytometry to analyse key EV and apolipoprotein markers. Our null hypothesis being that changes in the lipid and cholesterol profile in blood plasma has no effect on circulating EVs. At baseline, only

PCSK9$^{-/-}$ mice showed a significant decrease in ApoB compared to WT mice. Interestingly, when compared to WT animals, annexin V and CD63 levels increased significantly in both LDLR$^{-/-}$ and PCSK9$^{-/-}$ mice following HFD and at older age, despite the inverse relationship in cholesterol levels between the two KO models. We also observed that annexin V, CD63, and CD81 levels decreased across all mouse models after HFD. This trend was further confirmed when data from all groups were combined, revealing a significant decline in annexin V and CD63 levels post-HFD. These findings show clear evidence of an inverse relationship between EVs and lipoproteins, particularly LDL levels in mice.

One possible explanation is that elevated lipoprotein levels increase interactions between lipoproteins and annexin V/CD63-positive EVs, these interactions may induce greater cellular uptake of the EV-lipoprotein complexes through LDLR. EVs might also "piggyback" on LDL for uptake, reducing their levels in a lipoprotein-rich environment. Being that lipoproteins are magnitudes of order higher than EVs in circulation (82), this would allow for excessive binding and uptake of EVs via the lipoprotein's endocytic pathways. One interesting finding here, despite having higher cholesterol levels, LDLR$^{-/-}$ mice post-HFD and at old age maintained EV levels similar to PCSK9$^{-/-}$ mice at similar time points. This could be due to the involvement of alternative lipoprotein receptors, such as Lectin-like Oxidized Low-Density Lipoprotein Receptor-1 (LOX-1), Scavenger Receptor Class B Type 1 (SCARB-1), or Lipoprotein Receptor-related Protein-1 (LRP1), compensating in the absence of the LDLR and mediating the uptake of lipoproteins in LDLR$^{-/-}$ mice and these other receptors may not be as effective at uptake of EV-LDL complexes.

It is important to also note that EV levels were reduced within each mouse group, both after HFD and at old age. The different genetic backgrounds of the KO mice, although inversely related in terms of LDL-C levels, may not necessarily be inversely related in other diseases. Considering this, it is possible that PCSK9 inhibition or full knock-out may not always be in the best interest of the patient. If other ailments are present in the background that may be negatively affected by the lack of PCSK9 (53, 83) such as diebetes, this can rapidly deteriate the patients condition. It is indeed possible that some patients with very obscure genetic mutations or particular dietary habits may have elevated cholesterol levels without particular health detriments. Perhaps EVs in such

patients may be unaffected. To fully elucidate this, more work is needed on this topic to better understand the variation in EV levels and their relationship to disease in animal models and in a clinical setting. It has already been shown in other research that diet may be the root cause of hypercholesterolaemia, where in a second patient diet the same or similar diet will not have the same effect (84).

In line with *in vivo* testing, data from human samples reflected the findings observed in mouse models. We observed a similar decline in EV levels in humans with elevated cholesterol and lipoprotein levels. Specifically, our data revealed a statistically significant reduction in circulating CD63+ lEVs in hypercholesterolemic patients compared to normocholesterolemic individuals. However, unlike in the mouse models, the decrease in annexin V+ lEV levels in hypercholesterolemic patients were not significant. Overall, these findings align with our hypothesis of a connection between circulating EV levels and cholesterol and show that circulating CD63+ lEVs are inversely related to plasma LDL levels.

Despite the similarities in the relationship between EVs and lipoproteins, the lipoprotein landscape of mice is somewhat different than that of humans, and the development of atherosclerotic development in turn is vastly different between our species (63). This makes it difficult to drew clinical conclusions from our mouse model experiments. We do show however, that in the $LDLR^{-/-}$ group, mice had a relatively abundant circulating CD63+ lEV level at baseline (11-weeks old) and after (12 weeks) HFD with relatively low (similar to young WT mice) plaque levels. Once reaching old age (22-months), mice had developed plaques and CD63+ lEV levels were significantly reduced. This does indicate an inverse relationship (at least in mice) between atherosclerosis development and CD63+ lEVs. In humans MI occurrences predominantly stem from a sclerotic build-up in the coronary artery, while mice develop plaques principally in the root of the aortic arch (63) making mice cases of MI virtually non-existent. Subsequently to model MI in mice, it must be induced, with either the use of drugs, gene editing, or with surgical intervention (85, 86). Due to this distinction, as well as other differences in mice (87), it is challenging to hypothesise without additional studies as to the direct function EVs might play in the human progression of atherosclerosis and more specifically ACVD development. Based on the current knowledge of genesis and progression of atherosclerosis we have long known that inflammation plays an important role in

initiation and leads to exacerbation of the condition (88). We therefore made the decision to isolate IEVs from patients, this allowed us to examine whether EVs from hypercholesterolaemic patients may cause inflammation in healthy tissue.

The test was carried out by incubating these EVs with HUVECs. As shown in Figure 21, gene expression of CD36 and PPARγ increased specifically in HUVECs incubated with lEVs derived from hypercholesterolemic patients and not in those incubated with lEVs from control patients. Furthermore, we observe a reduction in the expression of VEGFA, again only from HUVECs incubated with hypercholesterolemic patients' EVs. we can also see an upregulation of CD36 which is in line with pro-inflammatory responses in both adipocytes and macrophages (89). In contrast, PPARγ has been associated with anti-inflammatory effects, mainly through its inhibition of TNFα (90) while VEGFA plays a role in pro-inflammatory processes (91). Here we see an up-regulation of PPARγ and a down- regulation of VEGFA in HUVECs incubated with the same EVs which suggest that EVs may play a more complex role in inflammation than initially postulated.

There are several known pathways by which EVs are endocytosed into cells. An early review (14) in the field of EV research already summarizes studies showing that phagocytosis and lipid raft endocytosis are used by cells to take up EVs. This 2014 (14) review even gives relatively a detailed account of clathrin and caveolin mediated EV endocytosis, with the suggestion that micropinocytosis also may be used by cells. Since then, later work shows the fusion of certain EVs with the cell membrane thereby depositing the EV cargo into recipient cells (92). It is also worth noting that EVs released during disease states carry markers of the processes involved in disease progression (93). Therefore, EVs released during disease states may contain markers to specifically target particular cells and certain tissue types. Much of the current data suggest that most EV uptake occurs as whole EVs endocytosed, with the EVs heading for the cell's endosomal compartments (94). We propose that EVs isolated from patients' PFP were endocytosed into HUVECs using a combination of the uptake methods discussed in earlier publications.

To better understand this inverse relationship with EVs and LDL, we can look at earlier publications. It has already been established that LDL and EVs associate in blood (44) and more recently it has become more accepted that EVs contain a protein corona on their

surface (95) and that within protein rich bodily fluids (such as blood) they will bind cholesterol. Our findings suggest that EVs might be cleared from circulation more efficiently when associated with lipoprotein particles. In individuals with elevated circulating cholesterol, these LDL-EV associations are likely to become more prevalent. An alternative explanation for this observation could be reduced cellular activity of platelets or monocytes (as well as other cell types) in disease states, leading to lower EV production and secretion. In addition to our research, a recent study has reported significant structural changes in EVs and alterations in their protein interactions after being released from cardiomyocytes exposed to high cholesterol treatments in rats (96). This finding brings further evidence to EV involvement in ACVD, but more specifically to the effects that hypercholesterolaemia has on EVs. These structural alterations to EVs could be what induced inflammatory responses in HUVECs when incubated with hypercholesterolaemic patient serum isolates.

Being that overall EV levels are shown to be reduced in patient with elevated cholesterol and mice with both elevated cholesterol and at old age, suggests a link to reduced cellular production of EVs. It is well established that cellular metabolism is reduced during aging (97, 98) as well as in certain disease states. EV production and secretion is part of the cell's normal metabolism, therefore reduction in metabolism and cell division can lead to reduced cellular output of EVs. It is also known that in other disease states such as oncogenic pathways where cellular replication and metabolism is increased with tumour growth, circulating EV levels are increased (99). In hypercholesterolaemia patients, however, there is not necessarily a clear pathway to reduced metabolism or overall reduction in cell replication. Therefore, the inverse relationship between LDL-C and EVs may still be linked to the association and co-endocytosis of the two particles into cells.

As is often the case with blood biomarkers, circulating cholesterol levels change post prandial (100, 101) in both healthy and diseased state patients. Our data (Figure 17) shows that contrary to cholesterol, CD63+ lEV levels do not shift significantly in fasting animals to those during normal prandial. This finding brings additional data to support our case in favour of the use of gated CD63+ events as an additional marker in the tracking of disease progression in relation to vascular diseases. Health professionals would be remiss not to mention that some patients may not be fasting as instructed before screenings. With this in mind, CD63 levels as mentioned above will seemingly not discriminate between fasted

and non-fasting patients. Making lEV measurements perhaps a more dependable and reproducible method of ACVD screening in a clinical setting.

Previous work has shown that platelet makers such as, CD41b, CD42a, and CD62P are abundantly found in sEVs isolated from human PFP (102). In the present work we show similar finding, only this time in lEVs and not only in human samples, but also from mice PFP. Although the classic EV Tetraspanin markers are universally known as CD9, CD63, and CD81, we observed other prominent markers more prevalent in both mice and human circulating EVs. Using the exosome bead based assay, we also spotted a positive correlation between CD29, CD42a, CD49e, and perhaps CD62P and LDL-C, while CD61 is inversley related to LDL-C.

Based on our results, one thing we can answer, is that specifically lEVs which stain positive for CD63+, can guide clinicians as to the cholesterol levels and regulation of their patients. Raised LDL-C and TC levels as stand-alone do not necessarily lead to cardiovascular diseases and are not used as standalone diagnostic markers for ACVD. Our data shown in Figure 17 also indicate that EV levels can be studied independently of certain lipoproteins. Further exploration of EV profiles could enhance our understanding and knowledge of cardiovascular health. This could lead to more precise prognostic tools and improved patient care and outcomes for individuals with elevated cholesterol levels.

Our data points at three key findings. Firstly, lEVs and primarily CD63+ lEVs are inversely related to cholesterol levels. The second key finding, CD63+ lEVs maybe inversely related to atherosclerosis. The third and final key finding is that circulating CD63+ lEV levels may become somewhat depleted with age. These findings are summarized in the abstract figure, Figure 22 below.

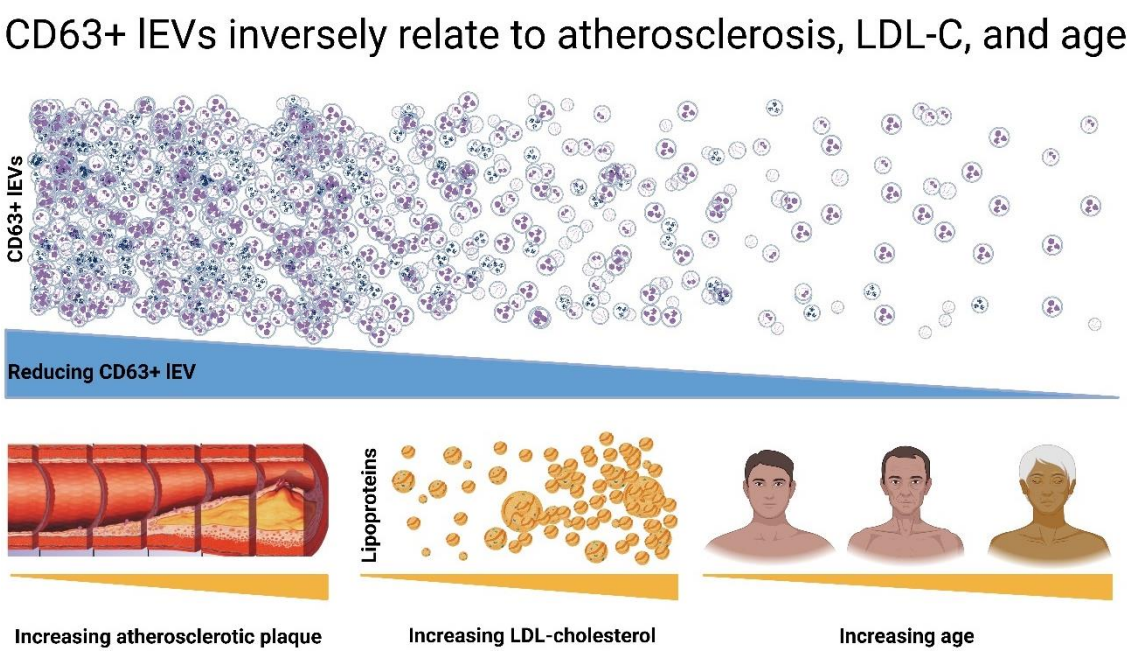

Figure 22. An abstract figure which summarises the findings shared in this thesis along with its associated publication. The top half of the figure shows extracellular vesicles (EVs), representing CD63+ large-EVs. Going from left to right these EV levels gradually become depleted as varying health states begin to deteriorate. The bottom left of the image shows increasing levels of atherosclerosis, where EV levels begin depletion with pathological progress. in the bottom centre, LDL- cholesterol levels begin to increase in the stages of dys-cholesterolaemia. Here too, EV levels begin to decline. In the bottom right, increasing age is represented. In an aging population, EV levels are also shown to reduce.

Based on the key findings of the current study, it seems evident that there would be the potential for CD63+ lEVs to be used as prognostically relevant markers in CVD. However, as seen with aging mice, these levels are inversely related to age as well as cardiovascular health. Perhaps with the use of an age index, it may be a good future tool alongside cholesterol levels as patient risk assessment for ACVD. One big advantage, is the lack of change in lEV levels during fasting, this this would enhance prognostics with less reliance on patient compliance.

Flow cytometers such as the FACSLyric™ from BD biosystems, or others, which are certified for in vitro diagnostics (IVD) can be implemented clinically, with the use of EV antibody staining alongside appropriate gating strategies. With the implementation of

newly available testing, patients may be able to receive more appropriate care for CVD with a more accurate screening.

6. Conclusions:

- EVs particularly CD63+ lEVs, show an inverse relationship with cholesterol levels, primarily LDL-C in mice and humans.

- CD63+ lEVs are also shown to be inversely associated with atherosclerosis in mice.

- Circulating levels of CD63+ lEVs tend to decline with age (particularly shown in the mouse model).

- Although circulating CD63+ lEVs levels appear to reduce with both advancing age and deteriorating cardiovascular health, which could limit their interpretability, we believe CD63+ lEVs exhibit strong potential as a prognostic marker in CVD.

This study serves a baseline which identified CD63+ lEVs as one (of perhaps several) EV population(s) in circulation linked to dyscholesterolaemia and elevated LDL levels in both mice and humans. In the future, expanding on the current study to a full scale clinical investigation could have a large beneficial impact on the evaluation of ACVD patients. With the use of a clinically approved flow cytometer, for instance the FACSLyric™ from BD biosystems, we can more robustly obtain patient EV levels. Here, we could use a sizable group of healthy young adults to serve as a baseline for plasma levels CD63+ lEVs as well as a larger number of patients with clinical hypercholesterolaemia, forming the basis of a clinical research project. Additionally, we could use patients of different age groups in an effort to identify an age-index of CD63+ lEV levels. The study can be broadened to include patience of both sexes establishing whether CD63+ lEV levels are translatable to female as well as male patients. The investigation may also be expanded upon with the inclusion of other markers, for instance the EV subpopulation CD9 can be supplemented, plus an additional investigation into sEV levels.

7. Summary:

In 2016 the discovery was made that EVs, and lipoproteins associate in blood plasma. After that initial discovery was made, many papers began flooding the field showing a co-isolation and contamination of lipoproteins in all EV preps from body fluids. The same was true for lipoprotein preparations, leading to researchers in lipoproteins taking a keen interest in the rapidly developing EV field. This prompted our hypothesis that EVs may play a crucial role in dyscholesterolaemia and ultimately in the development of atherosclerosis in CVD. Our research set out using 2 genetic mouse models ($PCSK9^{-/-}$ and $LDLR^{-/-}$) to simulate up and down regulated LDL levels respectively. Here we measured mice cholesterol and EV levels at baseline of 11-weeks old and again after either fed them HFD for 12 weeks or let them age to 22-months. In order to see how cholesterol levels might affect CVD in mice, we also measured cardiovascular function using Doppler ultrasound and measured plaques on the aortic arch using O-Red-O staining at all three time points. We also measured EVs levels in clinical samples of angina patients admitted to an emergency clinic, all of whom were eventually determined to be non-ischemic patients. We divided the clinical samples into 2 groups, group 1 with normocholesterolaemia and group 2 were those hypercholesterolaemia. Our results show $PCSK9^{-/-}$ have significantly lower TC and LDL levels where as $LDLR^{-/-}$ have significantly elevated TC and LDL levels at all time point. Our results show for the first time that annexin V and CD63 positive EVs inversely related to cholesterol in mice, and that CD63 positive EVs are inversely related cholesterol in humans. We also highlight that in mice, during feeding, cholesterol levels are elevated compared to fasted animals, this is consistent with previous studies in mice and humans. Interesting though lEV levels were stagnant whether animals were feeding or fasting. We also observe a cardioprotective element $PCSK9^{-/-}$ has on younger mice with HFD and that $LDLR^{-/-}$ causes plaque build-up in the long run. An additional finding here, $PCSK9^{-/-}$ mice have consistently greater body mass than WT mice. Together these results demonstrate an involvement of EVs in cholesterol dysfunction and propose CD63 positive lEV as an additional marker for ACVD. Showing consistently that CD63 positive lEV are inversely related to cholesterol levels in disease and pre-disease states in both mice and humans. We also highlight caution to patients on PCSK9 inhibitors, as weight gain and obesity become increasingly likely.

8. References:

1. Dasagrandhi D, Muthuswamy A, Swaminathan JK. Atherosclerosis: nexus of vascular dynamics and cellular cross talks. Molecular and Cellular Biochemistry. 2022:1-14,

2. Simonetto C, Heier M, Peters A, Kaiser JC, Rospleszcz S. From atherosclerosis to myocardial infarction: a process-oriented model investigating the role of risk factors. American Journal of Epidemiology. 2022;191(10):1766-1775,

3. Mortensen MB, Nordestgaard BG. Elevated LDL cholesterol and increased risk of myocardial infarction and atherosclerotic cardiovascular disease in individuals aged 70–100 years: a contemporary primary prevention cohort. The Lancet. 2020;396(10263):1644-1652,

4. Chen Y, Wright N, Guo Y, Turnbull I, Kartsonaki C, Yang L, Bian Z, Pei P, Pan D, Zhang Y. Mortality and recurrent vascular events after first incident stroke: a 9-year community-based study of 0· 5 million Chinese adults. The Lancet Global Health. 2020;8(4):e580-e590,

5. Jaramillo EA, Smith EJT, Matthay ZA, Sanders KM, Hiramoto JS, Gasper WJ, Conte MS, Iannuzzi JC. Racial and ethnic disparities in major adverse limb events persist for chronic limb threatening ischemia despite presenting limb threat severity after peripheral vascular intervention. J Vasc Surg. 2023;77(3):848-857 e2.10.1016/j.jvs.2022.10.043

6. Guo Y, Yan B, Gui Y, Tang Z, Tai S, Zhou S, Zheng XL. Physiology and role of PCSK9 in vascular disease: Potential impact of localized PCSK9 in vascular wall. J Cell Physiol. 2021;236(4):2333-2351.10.1002/jcp.30025

7. Wang N, Fulcher J, Abeysuriya N, Park L, Kumar S, Di Tanna GL, Wilcox I, Keech A, Rodgers A, Lal S. Intensive LDL cholesterol-lowering treatment beyond current recommendations for the prevention of major vascular events: a systematic review and meta-analysis of randomised trials including 327 037 participants. Lancet Diabetes Endocrinol. 2020;8(1):36-49.10.1016/S2213-8587(19)30388-2

8. Mertz DP. ["Atherosclerosis-index" (LDL/HDL): risk indicator in lipid metabolism disorders]. Med Klin. 1980;75(4):159-161, https://www.ncbi.nlm.nih.gov/pubmed/7374617

9. Anichkov NN, Chalatov S. Uber experimentelle cholesterinsteatose und ihre bedeuntung fur die entstehung einiger pathologischer prozess. Zentralbl Allg Pathol. 1913;24:1-9,

10. Wang B, Tang X, Yao L, Wang Y, Chen Z, Li M, Wu N, Wu D, Dai X, Jiang H. Disruption of USP9X in macrophages promotes foam cell formation and atherosclerosis. The Journal of Clinical Investigation. 2022;132(10),

11. Nagelkerke A, Ojansivu M, van der Koog L, Whittaker TE, Cunnane EM, Silva AM, Dekker N, Stevens MM. Extracellular vesicles for tissue repair and regeneration: Evidence, challenges and opportunities. Adv Drug Deliv Rev. 2021;175:113775.10.1016/j.addr.2021.04.013

12. Buzas EI. The roles of extracellular vesicles in the immune system. Nat Rev Immunol. 2023;23(4):236-250.10.1038/s41577-022-00763-8

13. Zhang Y, Kim JS, Wang TZ, Newton RU, Galvao DA, Gardiner RA, Hill MM, Taaffe DR. Potential Role of Exercise Induced Extracellular Vesicles in Prostate Cancer Suppression. Front Oncol. 2021;11:746040.10.3389/fonc.2021.746040

14. Mulcahy LA, Pink RC, Carter DR. Routes and mechanisms of extracellular vesicle uptake. J Extracell Vesicles. 2014;3.10.3402/jev.v3.24641

15. Chen P, Wang L, Fan X, Ning X, Yu B, Ou C, Chen M. Targeted delivery of extracellular vesicles in heart injury. Theranostics. 2021;11(5):2263-2277.10.7150/thno.51571

16. Welsh JA, Goberdhan DCI, O'Driscoll L, Buzas EI, Blenkiron C, Bussolati B, Cai H, Di Vizio D, Driedonks TAP, Erdbrugger U, Falcon-Perez JM, Fu QL, Hill AF, Lenassi M, Lim SK, Mahoney MG, Mohanty S, Moller A, Nieuwland R, Ochiya T, Sahoo S, Torrecilhas AC, Zheng L, Zijlstra A, Abuelreich S, Bagabas R, Bergese P, Bridges EM, Brucale M, Burger D, Carney RP, Cocucci E, Crescitelli R, Hanser E, Harris AL, Haughey NJ, Hendrix A, Ivanov AR, Jovanovic-Talisman T, Kruh-Garcia NA, Ku'ulei-Lyn Faustino V, Kyburz D, Lasser C, Lennon KM, Lotvall J, Maddox AL, Martens-Uzunova ES, Mizenko RR, Newman LA, Ridolfi A, Rohde E, Rojalin T, Rowland A, Saftics A, Sandau US, Saugstad JA, Shekari F, Swift S, Ter-Ovanesyan D, Tosar JP, Useckaite Z, Valle F, Varga Z, van der Pol E, van Herwijnen MJC, Wauben MHM, Wehman AM, Williams S, Zendrini A, Zimmerman AJ, Consortium M, Thery C, Witwer KW. Minimal

information for studies of extracellular vesicles (MISEV2023): From basic to advanced approaches. J Extracell Vesicles. 2024;13(2):e12404.10.1002/jev2.12404

17. Thery C, Witwer KW, Aikawa E, Alcaraz MJ, Anderson JD, Andriantsitohaina R, Antoniou A, Arab T, Archer F, Atkin-Smith GK, Ayre DC, Bach JM, Bachurski D, Baharvand H, Balaj L, Baldacchino S, Bauer NN, Baxter AA, Bebawy M, Beckham C, Bedina Zavec A, Benmoussa A, Berardi AC, Bergese P, Bielska E, Blenkiron C, Bobis-Wozowicz S, Boilard E, Boireau W, Bongiovanni A, Borras FE, Bosch S, Boulanger CM, Breakefield X, Breglio AM, Brennan MA, Brigstock DR, Brisson A, Broekman ML, Bromberg JF, Bryl-Gorecka P, Buch S, Buck AH, Burger D, Busatto S, Buschmann D, Bussolati B, Buzas EI, Byrd JB, Camussi G, Carter DR, Caruso S, Chamley LW, Chang YT, Chen C, Chen S, Cheng L, Chin AR, Clayton A, Clerici SP, Cocks A, Cocucci E, Coffey RJ, Cordeiro-da-Silva A, Couch Y, Coumans FA, Coyle B, Crescitelli R, Criado MF, D'Souza-Schorey C, Das S, Datta Chaudhuri A, de Candia P, De Santana EF, De Wever O, Del Portillo HA, Demaret T, Deville S, Devitt A, Dhondt B, Di Vizio D, Dieterich LC, Dolo V, Dominguez Rubio AP, Dominici M, Dourado MR, Driedonks TA, Duarte FV, Duncan HM, Eichenberger RM, Ekstrom K, El Andaloussi S, Elie-Caille C, Erdbrugger U, Falcon-Perez JM, Fatima F, Fish JE, Flores-Bellver M, Forsonits A, Frelet-Barrand A, Fricke F, Fuhrmann G, Gabrielsson S, Gamez-Valero A, Gardiner C, Gartner K, Gaudin R, Gho YS, Giebel B, Gilbert C, Gimona M, Giusti I, Goberdhan DC, Gorgens A, Gorski SM, Greening DW, Gross JC, Gualerzi A, Gupta GN, Gustafson D, Handberg A, Haraszti RA, Harrison P, Hegyesi H, Hendrix A, Hill AF, Hochberg FH, Hoffmann KF, Holder B, Holthofer H, Hosseinkhani B, Hu G, Huang Y, Huber V, Hunt S, Ibrahim AG, Ikezu T, Inal JM, Isin M, Ivanova A, Jackson HK, Jacobsen S, Jay SM, Jayachandran M, Jenster G, Jiang L, Johnson SM, Jones JC, Jong A, Jovanovic-Talisman T, Jung S, Kalluri R, Kano SI, Kaur S, Kawamura Y, Keller ET, Khamari D, Khomyakova E, Khvorova A, Kierulf P, Kim KP, Kislinger T, Klingeborn M, Klinke DJ, 2nd, Kornek M, Kosanovic MM, Kovacs AF, Kramer-Albers EM, Krasemann S, Krause M, Kurochkin IV, Kusuma GD, Kuypers S, Laitinen S, Langevin SM, Languino LR, Lannigan J, Lasser C, Laurent LC, Lavieu G, Lazaro-Ibanez E, Le Lay S, Lee MS, Lee YXF, Lemos DS, Lenassi M, Leszczynska A, Li IT, Liao K, Libregts SF, Ligeti E, Lim R, Lim SK, Line A, Linnemannstons K, Llorente A, Lombard CA, Lorenowicz MJ, Lorincz AM, Lotvall J, Lovett J, Lowry MC, Loyer X, Lu Q, Lukomska B, Lunavat TR, Maas SL, Malhi H,

Marcilla A, Mariani J, Mariscal J, Martens-Uzunova ES, Martin-Jaular L, Martinez MC, Martins VR, Mathieu M, Mathivanan S, Maugeri M, McGinnis LK, McVey MJ, Meckes DG, Jr., Meehan KL, Mertens I, Minciacchi VR, Moller A, Moller Jorgensen M, Morales-Kastresana A, Morhayim J, Mullier F, Muraca M, Musante L, Mussack V, Muth DC, Myburgh KH, Najrana T, Nawaz M, Nazarenko I, Nejsum P, Neri C, Neri T, Nieuwland R, Nimrichter L, Nolan JP, Nolte-'t Hoen EN, Noren Hooten N, O'Driscoll L, O'Grady T, O'Loghlen A, Ochiya T, Olivier M, Ortiz A, Ortiz LA, Osteikoetxea X, Ostergaard O, Ostrowski M, Park J, Pegtel DM, Peinado H, Perut F, Pfaffl MW, Phinney DG, Pieters BC, Pink RC, Pisetsky DS, Pogge von Strandmann E, Polakovicova I, Poon IK, Powell BH, Prada I, Pulliam L, Quesenberry P, Radeghieri A, Raffai RL, Raimondo S, Rak J, Ramirez MI, Raposo G, Rayyan MS, Regev-Rudzki N, Ricklefs FL, Robbins PD, Roberts DD, Rodrigues SC, Rohde E, Rome S, Rouschop KM, Rughetti A, Russell AE, Saa P, Sahoo S, Salas-Huenuleo E, Sanchez C, Saugstad JA, Saul MJ, Schiffelers RM, Schneider R, Schoyen TH, Scott A, Shahaj E, Sharma S, Shatnyeva O, Shekari F, Shelke GV, Shetty AK, Shiba K, Siljander PR, Silva AM, Skowronek A, Snyder OL, 2nd, Soares RP, Sodar BW, Soekmadji C, Sotillo J, Stahl PD, Stoorvogel W, Stott SL, Strasser EF, Swift S, Tahara H, Tewari M, Timms K, Tiwari S, Tixeira R, Tkach M, Toh WS, Tomasini R, Torrecilhas AC, Tosar JP, Toxavidis V, Urbanelli L, Vader P, van Balkom BW, van der Grein SG, Van Deun J, van Herwijnen MJ, Van Keuren-Jensen K, van Niel G, van Royen ME, van Wijnen AJ, Vasconcelos MH, Vechetti IJ, Jr., Veit TD, Vella LJ, Velot E, Verweij FJ, Vestad B, Vinas JL, Visnovitz T, Vukman KV, Wahlgren J, Watson DC, Wauben MH, Weaver A, Webber JP, Weber V, Wehman AM, Weiss DJ, Welsh JA, Wendt S, Wheelock AM, Wiener Z, Witte L, Wolfram J, Xagorari A, Xander P, Xu J, Yan X, Yanez-Mo M, Yin H, Yuana Y, Zappulli V, Zarubova J, Zekas V, Zhang JY, Zhao Z, Zheng L, Zheutlin AR, Zickler AM, Zimmermann P, Zivkovic AM, Zocco D, Zuba-Surma EK. Minimal information for studies of extracellular vesicles 2018 (MISEV2018): a position statement of the International Society for Extracellular Vesicles and update of the MISEV2014 guidelines. J Extracell Vesicles. 2018;7(1):1535750.10.1080/20013078.2018.1535750

18. Lotvall J, Hill AF, Hochberg F, Buzas EI, Di Vizio D, Gardiner C, Gho YS, Kurochkin IV, Mathivanan S, Quesenberry P, Sahoo S, Tahara H, Wauben MH, Witwer KW, Thery C. Minimal experimental requirements for definition of extracellular vesicles

and their functions: a position statement from the International Society for Extracellular Vesicles. J Extracell Vesicles. 2014;3:26913.10.3402/jev.v3.26913

19. Seo GM, Lee H, Kang YJ, Kim D, Sung JH. Development of in vitro model of exosome transport in microfluidic gut-brain axis-on-a-chip. Lab Chip. 2024;24(19):4581-4593.10.1039/d4lc00490f

20. Anastasi F, Botto A, Immordino B, Giovannetti E, McDonnell LA. Proteomics analysis of circulating small extracellular vesicles: Focus on the contribution of EVs to tumor metabolism. Cytokine Growth Factor Rev. 2023;73:3-19.10.1016/j.cytogfr.2023.08.003

21. Teo KYW, Tan R, Wong KL, Hey DHW, Hui JHP, Toh WS. Small extracellular vesicles from mesenchymal stromal cells: the next therapeutic paradigm for musculoskeletal disorders. Cytotherapy. 2023;25(8):837-846.10.1016/j.jcyt.2023.04.011

22. Shi B, Phan TK, Poon IKH. Extracellular vesicles from the dead: the final message. Trends Cell Biol. 2024.10.1016/j.tcb.2024.09.005

23. Brezgin S, Danilik O, Yudaeva A, Kachanov A, Kostyusheva A, Karandashov I, Ponomareva N, Zamyatnin Jr AA, Parodi A, Chulanov V, Kostyushev D. Basic guide for approaching drug delivery with extracellular vesicles. International Journal of Molecular Sciences. 2024 Sep 27;25(19):10401.

24. Couch Y, Buzàs EI, Di Vizio D, Gho YS, Harrison P, Hill AF, Lötvall J, Raposo G, Stahl PD, Théry C. A brief history of nearly EV-erything–The rise and rise of extracellular vesicles. Journal of extracellular vesicles. 2021;10(14):e12144,

25. Osteikoetxea X, Németh A, Sódar BW, Vukman KV, Buzás EI. Extracellular vesicles in cardiovascular disease: are they Jedi or Sith? The Journal of physiology. 2016;594(11):2881-2894,

26. Valcz G, Újvári B, Buzás EI, Krenács T, Spisák S, Kittel Á, Tulassay Z, Igaz P, Takács I, Molnár B. Small extracellular vesicle DNA-mediated horizontal gene transfer as a driving force for tumor evolution: Facts and riddles. Frontiers in Oncology. 2022;12:945376,

27. Szvicsek Z, Oszvald Á, Szabó L, Sándor GO, Kelemen A, Soós AÁ, Pálóczi K, Harsányi L, Tölgyes T, Dede K. Extracellular vesicle release from intestinal organoids is modulated by Apc mutation and other colorectal cancer progression factors. Cellular and Molecular Life Sciences. 2019;76:2463-2476,

28. Srivastava A, Rathore S, Munshi A, Ramesh R. Extracellular vesicles in oncology: from immune suppression to immunotherapy. The AAPS Journal. 2021;23:1-15,

29. Jansen F, Li Q, Pfeifer A, Werner N. Endothelial-and immune cell-derived extracellular vesicles in the regulation of cardiovascular health and disease. Basic to Translational Science. 2017;2(6):790-807,

30. Osteikoetxea X, Silva A, Lázaro-Ibáñez E, Salmond N, Shatnyeva O, Stein J, Schick J, Wren S, Lindgren J, Firth M. Engineered Cas9 extracellular vesicles as a novel gene editing tool. Journal of extracellular vesicles. 2022;11(5):e12225,

31. Li X, La Salvia S, Liang Y, Adamiak M, Kohlbrenner E, Jeong D, Chepurko E, Ceholski D, Lopez-Gordo E, Yoon S. Extracellular Vesicle–Encapsulated Adeno-Associated Viruses for Therapeutic Gene Delivery to the Heart. Circulation. 2023;148(5):405-425,

32. Lv H, Feng Z, Chen X, Zhang Z, Zhou T, Wei J, Feng L, Tao Y, Chen F, Lu S. Global scientific trends on exosomes therapy for osteoporosis from 2004 to 2023: A bibliometric and visualized analysis. Medicine (Baltimore). 2024;103(28):e38835.10.1097/MD.0000000000038835

33. Susa F, Limongi T, Borgione F, Peiretti S, Vallino M, Cauda V, Pisano R. Comparative Studies of Different Preservation Methods and Relative Freeze-Drying Formulations for Extracellular Vesicle Pharmaceutical Applications. ACS Biomater Sci Eng. 2023;9(10):5871-5885.10.1021/acsbiomaterials.3c00678

34. Al-Jipouri A, Eritja A, Bozic M. Unraveling the Multifaceted Roles of Extracellular Vesicles: Insights into Biology, Pharmacology, and Pharmaceutical Applications for Drug Delivery. Int J Mol Sci. 2023;25(1).10.3390/ijms25010485

35. St-Amand R, Ngo Sock ÉT, Quinn S, Lavoie J-M, St-Pierre DH. Two weeks of western diet disrupts liver molecular markers of cholesterol metabolism in rats. Lipids in Health and Disease. 2020;19:1-11,

36. Saluja T, Davies A, Oldmeadow C, Boyle AJ. Impact of fast-food outlet density on incidence of myocardial infarction in the Hunter region. Internal Medicine Journal. 2021;51(2):243-248,

37. Guo N, Zhu Y, Tian D, Zhao Y, Zhang C, Mu C, Han C, Zhu R, Liu X. Role of diet in stroke incidence: an umbrella review of meta-analyses of prospective observational studies. BMC medicine. 2022;20(1):1-15,

38. Beena T, Jesil MA, Harikumar K. Cross-talk between AMP-activated protein kinase and the sonic hedgehog pathway in the high-fat diet triggered colorectal cancer. Archives of Biochemistry and Biophysics. 2023:109500,
39. Carson JAS, Lichtenstein AH, Anderson CA, Appel LJ, Kris-Etherton PM, Meyer KA, Petersen K, Polonsky T, Van Horn L. Dietary cholesterol and cardiovascular risk: a science advisory from the American Heart Association. Circulation. 2020;141(3):e39-e53,
40. Burén J, Ericsson M, Damasceno NRT, Sjödin A. A ketogenic low-carbohydrate high-fat diet increases LDL cholesterol in healthy, young, normal-weight women: a randomized controlled feeding trial. Nutrients. 2021;13(3):814,
41. Gabet A, Grave C, Bonaldi C, Blacher J, Olie V. Estimation of the proportion of cardiovascular disease cases in France attributable to high concentrations of low-density lipoprotein cholesterol. Arch Cardiovasc Dis. 2024.10.1016/j.acvd.2024.11.001
42. Xu S, Shiomi H, Yamashita Y, Koyama S, Horie T, Baba O, Kimura M, Nakashima Y, Sowa N, Hasegawa K. CRISPR-Cas9-guided amplification-free genomic diagnosis for familial hypercholesterolemia using nanopore sequencing. Plos one. 2024;19(3):e0297231,
https://www.ncbi.nlm.nih.gov/pmc/articles/PMC10954175/pdf/pone.0297231.pdf
43. Rogozik J, Główczyńska R, Grabowski M. Genetic backgrounds and diagnosis of familial hypercholesterolemia. Clinical Genetics. 2024;105(1):3-12,
44. Sódar BW, Kittel Á, Pálóczi K, Vukman KV, Osteikoetxea X, Szabó-Taylor K, Németh A, Sperlágh B, Baranyai T, Giricz Z. Low-density lipoprotein mimics blood plasma-derived exosomes and microvesicles during isolation and detection. Scientific reports. 2016;6(1):24316,
45. Merij LB, da Silva LR, Palhinha L, Gomes MT, Dib PRB, Martins-Goncalves R, Toledo-Quiroga K, Raposo-Nunes MA, Andrade FB, de Toledo Martins S, Nascimento ALR, Rocha VN, Alves LR, Bozza PT, de Oliveira Trugilho MR, Hottz ED. Density-based lipoprotein depletion improves extracellular vesicle isolation and functional analysis. J Thromb Haemost. 2024;22(5):1372-1388.10.1016/j.jtha.2024.01.010
46. Lozano-Andres E, Enciso-Martinez A, Gijsbers A, Ridolfi A, Van Niel G, Libregts S, Pinheiro C, van Herwijnen MJC, Hendrix A, Brucale M, Valle F, Peters PJ, Otto C, Arkesteijn GJA, Wauben MHM. Physical association of low density lipoprotein particles

and extracellular vesicles unveiled by single particle analysis. J Extracell Vesicles. 2023;12(11):e12376.10.1002/jev2.12376

47. Nemeth K, Kestecher BM, Ghosal S, Bodnar BR, Kittel A, Hambalko S, Kovacshazi C, Giricz Z, Ferdinandy P, Osteikoetxea X, Burkhardt R, Buzas EI, Orso E. Therapeutic and pharmacological applications of extracellular vesicles and lipoproteins. Br J Pharmacol. 2024;181(23):4733-4749.10.1111/bph.17336

48. Lin M, Li M, Zheng H, Sun H, Zhang J. Lipoprotein proteome profile: novel insight into hyperlipidemia. Clin Transl Med. 2021;11(4):e361.10.1002/ctm2.361

49. Toth EA, Turiak L, Visnovitz T, Cserep C, Mazlo A, Sodar BW, Forsonits AI, Petovari G, Sebestyen A, Komlosi Z, Drahos L, Kittel A, Nagy G, Bacsi A, Denes A, Gho YS, Szabo-Taylor KE, Buzas EI. Formation of a protein corona on the surface of extracellular vesicles in blood plasma. J Extracell Vesicles. 2021;10(11):e12140.10.1002/jev2.12140

50. Shi X, Chen Y, Liu Q, Mei X, Liu J, Tang Y, Luo R, Sun D, Ma Y, Wu W. LDLR dysfunction induces LDL accumulation and promotes pulmonary fibrosis. Clinical and Translational Medicine. 2022;12(1):e711,

51. Li Z, Zhao P, Zhang Y, Wang J, Wang C, Liu Y, Yang G, Yuan L. Exosome-based Ldlr gene therapy for familial hypercholesterolemia in a mouse model. Theranostics. 2021;11(6):2953,

52. Sun R, Peng M, Xu P, Huang F, Xie Y, Li J, Hong Y, Guo H, Liu Q, Zhu W. Low-density lipoprotein receptor (LDLR) regulates NLRP3-mediated neuronal pyroptosis following cerebral ischemia/reperfusion injury. Journal of neuroinflammation. 2020;17(1):1-17,

53. Pasta A, Cremonini AL, Pisciotta L, Buscaglia A, Porto I, Barra F, Ferrero S, Brunelli C, Rosa GM. PCSK9 inhibitors for treating hypercholesterolemia. Expert Opin Pharmacother. 2020;21(3):353-63.10.1080/14656566.2019.1702970

54. Guo Y, Yan B, Tai S, Zhou S, Zheng XL. PCSK9: Associated with cardiac diseases and their risk factors? Arch Biochem Biophys. 2021;704:108717.10.1016/j.abb.2020.108717

55. Pasta A, Cremonini AL, Pisciotta L, Buscaglia A, Porto I, Barra F, Ferrero S, Brunelli C, Rosa GM. PCSK9 inhibitors for treating hypercholesterolemia. Expert opinion on pharmacotherapy. 2020;21(3):353-363,

56. Jin J. PCSK9 Inhibitors for Treating High Cholesterol. JAMA. 2015;314(21):2320-,

57. Sahel DK, Vora LK, Saraswat A, Sharma S, Monpara J, D'Souza AA, Mishra D, Tryphena KP, Kawakita S, Khan S. CRISPR/Cas9 Genome Editing for Tissue-Specific In Vivo Targeting: Nanomaterials and Translational Perspective. Advanced Science. 2023:2207512,

58. Di Taranto MD, Giacobbe C, Fortunato G. Familial hypercholesterolemia: A complex genetic disease with variable phenotypes. European journal of medical genetics. 2020;63(4):103831,

59. Bianconi V, Banach M, Pirro M, Panel ILE. Why patients with familial hypercholesterolemia are at high cardiovascular risk? Beyond LDL-C levels. Trends in Cardiovascular Medicine. 2021;31(4):205-215,

60. Palanichamy K, Vadivalagan C, Fan Y-J. Isolation and purification of exosome and other extracellular vesicles. Extracellular Vesicles for Therapeutic and Diagnostic Applications: Elsevier; 2025. p. 1-23.

61. Kestecher BM, Nemeth K, Ghosal S, Sayour NV, Gergely TG, Bodnar BR, Forsonits AI, Sodar BW, Oesterreicher J, Holnthoner W, Varga ZV, Giricz Z, Ferdinandy P, Buzas EI, Osteikoetxea X. Reduced circulating CD63(+) extracellular vesicle levels associate with atherosclerosis in hypercholesterolaemic mice and humans. Cardiovasc Diabetol. 2024;23(1):368.10.1186/s12933-024-02459-w

62. Sayour NV, Tóth VÉ, Nagy RN, Vörös I, Gergely TG, Onódi Z, Nagy N, Bödör C, Váradi B, Ruppert M. Droplet Digital PCR Is a Novel Screening Method Identifying Potential Cardiac G-Protein-Coupled Receptors as Candidate Pharmacological Targets in a Rat Model of Pressure-Overload-Induced Cardiac Dysfunction. International Journal of Molecular Sciences. 2023;24(18):13826,

63. Centa M, Ketelhuth DF, Malin S, Gisterå A. Quantification of atherosclerosis in mice. JoVE (Journal of Visualized Experiments). 2019(148):e59828,

64. Lacroix R, Judicone C, Poncelet P, Robert S, Arnaud L, Sampol J, DIGNAT-GEORGE F. Impact of pre-analytical parameters on the measurement of circulating microparticles: towards standardization of protocol. Journal of Thrombosis and Haemostasis. 2012;10(3):437-446,

65. Lacroix R, Judicone C, Mooberry M, Boucekine M, Key NS, Dignat-George F. Standardization of pre-analytical variables in plasma microparticle determination: results of the International Society on Thrombosis and Haemostasis SSC Collaborative workshop. Journal of Thrombosis and Haemostasis. 2013;11(6):1190-1193,

66. Mhaimeed O, Burney ZA, Schott SL, Kohli P, Marvel FA, Martin SS. The Importance of LDL-C Lowering in Atherosclerotic Cardiovascular Disease Prevention: Lower for Longer is Better. American Journal of Preventive Cardiology. 2024:100649,

67. Kjeldsen EW, Nordestgaard LT, Frikke-Schmidt R. HDL cholesterol and non-cardiovascular disease: a narrative review. International Journal of Molecular Sciences. 2021;22(9):4547,

68. Trimarco V, Izzo R, Morisco C, Mone P, Virginia Manzi M, Falco A, Pacella D, Gallo P, Lembo M, Santulli G. High HDL (high-density lipoprotein) cholesterol increases cardiovascular risk in hypertensive patients. Hypertension. 2022;79(10):2355-2363,

69. Feng M, Darabi M, Tubeuf E, Canicio A, Lhomme M, Frisdal E, Lanfranchi-Lebreton S, Matheron L, Rached F, Ponnaiah M. Free cholesterol transfer to high-density lipoprotein (HDL) upon triglyceride lipolysis underlies the U-shape relationship between HDL-cholesterol and cardiovascular disease. European journal of preventive cardiology. 2020;27(15):1606-1616,

70. Panzoldo NB, Urban A, Parra ES, Oliveira R, Zago VS, da Silva LR, de Faria EC. Differences and similarities of postprandial lipemia in rodents and humans. Lipids in health and disease. 2011;10:1-4,

71. Baragetti A, Balzarotti G, Grigore L, Pellegatta F, Guerrini U, Pisano G, Fracanzani AL, Fargion S, Norata GD, Catapano AL. PCSK9 deficiency results in increased ectopic fat accumulation in experimental models and in humans. European journal of preventive cardiology. 2017;24(17):1870-1877,

72. Singh K, Gupta JK, Kumar S, Singh K, Meenakshi K, Kumar K. PCSK9 Inhibitors: Pharmacology and Therapeutic Potential. 2022,

73. Németh K, Tóth B, Sarnyai F, Koncz A, Lenzinger D, Kereszturi É, Visnovitz T, Kestecher BM, Osteikoetxea X, Csala M. High fat diet and PCSK9 knockout modulates lipid profile of the liver and changes the expression of lipid homeostasis related genes. Nutrition & Metabolism. 2023;20(1):1-14,

74. Demers A, Samami S, Lauzier B, Des Rosiers C, Sock ETN, Ong H, Mayer G. PCSK9 induces CD36 degradation and affects long-chain fatty acid uptake and triglyceride metabolism in adipocytes and in mouse liver. Arteriosclerosis, thrombosis, and vascular biology. 2015;35(12):2517-2525,

75. Fan FS. Small-interfering RNA targeting proprotein convertase subtilisin/kexin type 9 might promote fatty liver disease and hepatocellular carcinoma through upregulation of CD36. Tumor Biology. 2023;45(1):73-80,

76. Katzmann JL, Cupido AJ, Laufs U. Gene therapy targeting PCSK9. Metabolites. 2022;12(1):70,

77. Emmer C, Bosnjak M, Mata J. The association between weight stigma and mental health: A meta-analysis. Obesity Reviews. 2020;21(1):e12935,

78. Yanai S, Endo S. Functional aging in male C57BL/6J mice across the life-span: a systematic behavioral analysis of motor, emotional, and memory function to define an aging phenotype. Frontiers in aging neuroscience. 2021;13:697621,

79. Jung HN, Kim MJ, Kim HS, Lee WJ, Min SH, Kim YJ, Jung CH. Age-Related Associations of Low-Density Lipoprotein Cholesterol and Atherosclerotic Cardiovascular Disease: A Nationwide Population-Based Cohort Study. Journal of the American Heart Association. 2022;11(9):e024637,

80. Ueda P, Gulayin P, Danaei G. Long-term moderately elevated LDL-cholesterol and blood pressure and risk of coronary heart disease. PLoS One. 2018;13(7):e0200017.10.1371/journal.pone.0200017

81. Yuan C, Liu F, Huang K, Shen C, Li J, Liang F, Yang X, Cao J, Chen S, Hu D, Huang J, Liu Y, Lu X, Gu D. Association of Long-Term Exposure to Ambient Fine Particulate Matter with Atherosclerotic Cardiovascular Disease Incidence Varies across Populations with Different Predicted Risks: The China-PAR Project. Environ Sci Technol. 2023;57(27):9934-9942.10.1021/acs.est.3c01460

82. Simonsen JB. What Are We Looking At? Extracellular Vesicles, Lipoproteins, or Both? Circ Res. 2017;121(8):920-922.10.1161/CIRCRESAHA.117.311767

83. Baragetti A, Balzarotti G, Grigore L, Pellegatta F, Guerrini U, Pisano G, Fracanzani AL, Fargion S, Norata GD, Catapano AL. PCSK9 deficiency results in increased ectopic fat accumulation in experimental models and in humans. Eur J Prev Cardiol. 2017;24(17):1870-1877.10.1177/2047487317724342

84. Zhao B, Gan L, Graubard BI, Mannisto S, Albanes D, Huang J. Associations of Dietary Cholesterol, Serum Cholesterol, and Egg Consumption With Overall and Cause-Specific Mortality: Systematic Review and Updated Meta-Analysis. Circulation. 2022;145(20):1506-1520.10.1161/CIRCULATIONAHA.121.057642

85. Sun Q, Wang KK, Pan M, Zhou JP, Qiu XT, Wang ZY, Yang Z, Chen Y, Shen H, Gu QL, Fang LH, Zhang GG, Bai YP. A minimally invasive approach to induce myocardial infarction in mice without thoracotomy. J Cell Mol Med. 2018;22(11):5208-5219.10.1111/jcmm.13708

86. Jiang C, Chen J, Zhao Y, Gao D, Wang H, Pu J. A Modified Simple Method for Induction of Myocardial Infarction in Mice. J Vis Exp. 2021(178).10.3791/63042

87. Oppi S, Lüscher TF, Stein S. Mouse models for atherosclerosis research—which is my line? Frontiers in cardiovascular medicine. 2019:46,

88. Wei Y, Lan B, Zheng T, Yang L, Zhang X, Cheng L, Tuerhongjiang G, Yuan Z, Wu Y. GSDME-mediated pyroptosis promotes the progression and associated inflammation of atherosclerosis. Nat Commun. 2023;14(1):929.10.1038/s41467-023-36614-w

89. Kennedy DJ, Kuchibhotla S, Westfall KM, Silverstein RL, Morton RE, Febbraio M. A CD36-dependent pathway enhances macrophage and adipose tissue inflammation and impairs insulin signalling. Cardiovasc Res. 2011;89(3):604-613.10.1093/cvr/cvq360

90. Decara J, Rivera P, Lopez-Gambero AJ, Serrano A, Pavon FJ, Baixeras E, Rodriguez de Fonseca F, Suarez J. Peroxisome Proliferator-Activated Receptors: Experimental Targeting for the Treatment of Inflammatory Bowel Diseases. Front Pharmacol. 2020;11:730.10.3389/fphar.2020.00730

91. Scaldaferri F, Vetrano S, Sans M, Arena V, Straface G, Stigliano E, Repici A, Sturm A, Malesci A, Panes J, Yla-Herttuala S, Fiocchi C, Danese S. VEGF-A links angiogenesis and inflammation in inflammatory bowel disease pathogenesis. Gastroenterology. 2009;136(2):585-595 e5.10.1053/j.gastro.2008.09.064

92. Kwok ZH, Wang C, Jin Y. Extracellular Vesicle Transportation and Uptake by Recipient Cells: A Critical Process to Regulate Human Diseases. Processes (Basel). 2021;9(2).10.3390/pr9020273

93. French KC, Antonyak MA, Cerione RA. Extracellular vesicle docking at the cellular port: Extracellular vesicle binding and uptake. Semin Cell Dev Biol. 2017;67:48-55.10.1016/j.semcdb.2017.01.002

94. Joshi BS, de Beer MA, Giepmans BNG, Zuhorn IS. Endocytosis of Extracellular Vesicles and Release of Their Cargo from Endosomes. ACS Nano. 2020;14(4):4444-4455.10.1021/acsnano.9b10033

95. Tóth EÁ, Turiák L, Visnovitz T, Cserép C, Mázló A, Sódar BW, Försönits AI, Petővári G, Sebestyén A, Komlósi Z. Formation of a protein corona on the surface of extracellular vesicles in blood plasma. Journal of extracellular vesicles. 2021;10(11):e12140,

96. Kovacshazi C, Hambalko S, Sayour NV, Gergely TG, Brenner GB, Pelyhe C, Kapui D, Weber BY, Hultenschmidt AL, Pallinger E, Buzas EI, Zolcsak A, Kiss B, Bozo T, Csanyi C, Kosa N, Kellermayer M, Farkas R, Karvaly GB, Wynne K, Matallanas D, Ferdinandy P, Giricz Z. Effect of hypercholesterolemia on circulating and cardiomyocyte-derived extracellular vesicles. Sci Rep. 2024;14(1):12016.10.1038/s41598-024-62689-6

97. Han S, Georgiev P, Ringel AE, Sharpe AH, Haigis MC. Age-associated remodeling of T cell immunity and metabolism. Cell Metab. 2023;35(1):36-55.10.1016/j.cmet.2022.11.005

98. Maiese K. Cellular Metabolism: A Fundamental Component of Degeneration in the Nervous System. Biomolecules. 2023;13(5).10.3390/biom13050816

99. Ferguson S, Weissleder R. Modeling EV Kinetics for Use in Early Cancer Detection. Adv Biosyst. 2020;4(12):e1900305.10.1002/adbi.201900305

100. Craig SR, Amin RV, Russell DW, Paradise NF. Blood cholesterol screening: influence of fasting state on cholesterol results and management decisions. Journal of general internal medicine. 2000;15:395-399,

101. Chakraborty M, Singh P, Dsouza JM, Pethusamy K, Thatkar PV. Fasting and postprandial lipid parameters: A comparative evaluation of cardiovascular risk assessment in prediabetes and diabetes. Journal of Family Medicine and Primary Care. 2020;9(1):287,

102. Małys MS, Köller MC, Papp K, Aigner C, Dioso D, Mucher P, Schachner H, Bonelli M, Haslacher H, Rees AJ. Small extracellular vesicles are released ex vivo from

platelets into serum and from residual blood cells into stored plasma. Journal of Extracellular Biology. 2023;2(5):e88,

9 Bibliography of the candidate's publications

9.1. List of original publications within the topic of the PhD thesis:

Kestecher Brachyahu M, Németh Krisztina, Ghosal Sayam, Sayour Nabil V, Gergely Tamás G, Bodnár Bernadett R, Försönits András I, Sódar Barbara W, Oesterreicher Johannes, Holnthoner Wolfgang, Varga Zoltán V., Giricz Zoltán, Ferdinandy Péter, Buzás Edit I., Osteikoetxea Xabier
Reduced circulating CD63+ extracellular vesicle levels associate with atherosclerosis in hypercholesterolaemic mice and humans
CARDIOVASCULAR DIABETOLOGY 23 : 1 Paper: 368 , 14 p. (2024)
Scopus - Internal Medicine Rank: D1
IF: 8,5

9.2 List of original publications not relating to the topic of the PhD thesis:

Ghosal Sayam, Bodnár Bernadett, Kestecher Brachyahu Meir, Nagy Ákos, László Tamás, Yilmaz Bora, Zeng Yixuan, Szabó Adrienn, Bödör Csaba, Buzás Edit I, Osteikoetxea Xabier
Revolutionizing therapeutics: Unleashing the power of extracellular vesicles for disease intervention
CURRENT OPINION IN PHYSIOLOGY 43 Paper: 100815 , 11 p. (2025)
Scopus - Physiology (medical) Rank: Q2
IF: 2,5

Németh Krisztina, Kestecher Brachyahu M, Ghosal Sayam, Bodnár Bernadett R, Kittel Ágnes, Hambalkó Szabolcs, Kovácsházi Csenger, Giricz Zoltán, Ferdinandy Péter, Osteikoetxea Xabier, Burkhardt Ralph, Buzas Edit I, Orsó Evelyn
Therapeutic and pharmacological applications of extracellular vesicles and lipoproteins
BRITISH JOURNAL OF PHARMACOLOGY 181 : 23 pp. 4733-4749. (2024)
Publication: 35401823 | Survey paper (Journal Article) | Scientific
Scopus - Pharmacology Rank: D1
IF: 6,8

Welsh Joshua A, Goberdhan Deborah C I, O'Driscoll Lorraine, Buzas Edit I, Blenkiron

Cherie, Bussolati Benedetta, Cai Houjian, Di Vizio Dolores, Driedonks Tom A P, Erdbrügger Uta, Falcon-Perez Juan M, Fu Qing-Ling, Hill Andrew, Lenassi Metka, Lim Sai Kiang, Mahoney My G, Mohanty Sujata, Möller Andreas, Nieuwland Rienk, Ochiya Takahiro, Sahoo Susmita, Torrecilhas Ana C, Zheng Lei, Zijlstra Andries, Abuelreich Sarah, Bagabas Reem, Bergese Paolo, Bridges Esther M, Brucale Marco, Burger Dylan, Carney Randy P, Cocucci Emanuele, Colombo Federico, Crescitelli Rossella, ….. Kestecher Brachyahu M…et al
Minimal information for studies of extracellular vesicles (MISEV2023): From basic to advanced approaches
JOURNAL OF EXTRACELLULAR VESICLES 13 : 2 Paper: e12404 , 84 p. (2024)
Publication: 34567532 | Study Group (Journal Article) | Scientific
Scopus - Histology Rank: D1
IF: 15,5

Németh Krisztina, Tóth, Blanka, Sarnyai Farkas, Koncz Anna, Lenzinger Dorina, Kereszturi Éva, Visnovitz Tamás, Kestecher Brachyahu Meir, Osteikoetxea Xabier, Csala Miklós, Buzás Edit I, Tamási Viola
High fat diet and PCSK9 knockout modulates lipid profile of the liver and changes the expression of lipid homeostasis related genes
NUTRITION & METABOLISM 20 : 1 Paper: 19 , 14 p. (2023)
Publication: 33726492 |Article (Journal Article) | Scientific
Scopus - Nutrition and Dietetics Rank: Q1
IF: 3,9

The cumulative impact factor: IF: 37,2

10 Acknowledgements

I would like to express my gratitude and acknowledge all those who have helped with my project and helped me develop as a scientist over the last five years. In the HCEMM-SU-EV group I would like to thank Bodnár Bernadett, Sayam Ghosal, Adrienn Szabó, Barbara Sódar and my former student Yixuan Zeng.

I would like to give special thanks to András Försönits and Krisztina Németh from the Departments EV group for experimental help and experimental design support during my PhD. I would like to further thank all members of the EV group and indeed the entire Department of Genetics, Cells, and Immunobiology for their ongoing welcoming attitude and support during my research and training at the Department.

For their willingness, friendliness, and kindness and their support in collaboration (often with last minute notice) I would like to thank Tamás Gergely and Nabil Sayour. I would also like to acknowledge Zoltán Giricz, Zoltán V. Varga and Péter Ferdinandy for their support in experimental design, use of equipment, advice, and help with manuscript preparation.

I would also like to thank those from beyond our borders in Vienna Austria: Wolfgang Holnthoner and Johannes Oesterreicher for their collaboration, training and encouragement in my project.

I would also like to thank my parents, who have continued to support me through the long and winding road on my path to becoming who I am today. I am also deeply thankful to all my many siblings for all their continued support, words of wisdom and for always believing in me. For her ongoing invaluable advice and the pride she continues to show for me, I would also like to express my gratitude to my dear grandmother.

From her innovation and conceptualisation of my project to experimental design and help. For her ever sympathetic and inspiring outlook not just towards me, but indeed to our entire department, I would like to thank Professor Edit Buzás.

Finally, I owe a huge debt of gratitude to my PhD supervisor Dr Xabier Osteikoetxea whose guidance and support have been invaluable though the simplest and toughest times of my PhD. Without his supervision and guidance, I would not have been able to publish my work and defend my PhD.